ISSN 1063-7761, Journal of Experimental and Theoretical Physics, 2021, Vol. 132, No. 1, pp. 127–147. © Pleiades Publishing, Inc., 2021.
Russian Text © The Author(s), 2021, published in Zhurnal Eksperimental'noi i Teoreticheskoi Fiziki, 2021, Vol. 159, No. 1, pp. 150–175.

Spatiotemporal Regimes in the Kuramoto–Battogtokh System of Nonidentical Oscillators

M. I. Bolotov[a,*], L. A. Smirnov[a,b,], E. S. Bubnova[a], G. V. Osipov[a,***], and A. S. Pikovsky[c,a,****]**

[a] *Research and Education Mathematics Center "Mathematics of Future Technologies," Institute of Information Technologies, Mathematics, and Mechanics, Lobachevsky State University of Nizhny Novgorod, Nizhny Novgorod, 603950 Russia*

[b] *Institute of Applied Physics, Russian Academy of Sciences, Nizhny Novgorod, 603950 Russia*

[c] *Institute for Physics and Astronomy, University of Potsdam, Potsdam-Golm, D-14476 Germany*

**e-mail: maksim.bolotov@itmm.unn.ru*

***e-mail: smirnov_lev@appl.sci-nnov.ru*

****e-mail: osipov@vmk.unn.ru*

*****e-mail: pikovsky@uni-postdam.de*

Received August 11, 2020; revised August 11, 2020; accepted September 9, 2020

Abstract—We consider the spatiotemporal states of an ensemble of nonlocally coupled nonidentical phase oscillators, which correspond to different regimes of the long-term evolution of such a system. We have obtained homogeneous, twisted, and nonhomogeneous stationary solutions to the Ott–Antonsen equations corresponding to key variants of the realized collective rotational motion of elements of the medium in question with nonzero mesoscopic characteristics determining the degree of coherence of the dynamics of neighboring particles. We have described the procedures of the search for the class of nonhomogeneous solutions as stationary points of the auxiliary point map and of determining the stability based on analysis of the eigenvalue spectrum of the composite operator. Static and breather cluster regimes have been demonstrated and described, as well as the regimes with an irregular behavior of averaged complex fields including, in particular, the local order parameter.

DOI: 10.1134/S1063776121010106

1. INTRODUCTION

Systems of coupled oscillators are topical objects for theoretical and experimental investigations. This is primarily because such systems are basic models in various fields of modern science and technology. These systems are successfully used for describing not only mechanical objects (in particular, coupled pendulums [1, 2] and metronomes fixed on a common base [3, 4]), but also various processes in electrical (including power grid networks [5, 6], solid-state structures [7, 8], and molecular chains [9, 10]). References to specific experimental and theoretical investigations can be found, for example, in monographs [11, 12] and in review [13].

A number of key fundamental phenomena typical of nonlinear oscillator media of different origins can often be successfully analyzed using the phase approximation [12, 14, 15]. Such phenomena include, in particular, the synchronization and emergence of correlations in the system [1, 11]. A transition from more accurate and concrete theoretical formulations to a universal description based on dynamic equations for phase variables reveals universal principles and general regularities in the behavior of physical, chemical, biological, and social systems. The behavior of a population of oscillators interacting via the mean field is analyzed most often using the well-known Kuramoto model with global coupling and its various modifications [11, 13, 16–22]. A distinguishing feature of such a coupling topology is the absence of information on the position of elements of the ensemble in the coordinate space. For this reason, despite the possibility of combining oscillators into clusters, it is impossible in this case to formulate problems of the formation of spatial structures and the propagation of waves. However, the situation changes radically if the interaction in the medium is not global, but local by nature because the system becomes spatially ordered. Full symmetry relative to transposition of elements in such a system disappears automatically, and their numbering plays an important role in analysis of the dynamics of oscillator populations.

The nonlocal coupling can be represented analytically, for example, in the form of a convolution operator. The kernel of such an operator completely determines the type of the interaction in such an oscillator medium. In spite of the fact that among other things, the long-range interactions decreasing in accordance with a power law were also considered in the literature (see, for example, [23]), important and generally unexpected results were obtained for kernels with finite radii and with exponentially decreasing tails [24–26]. Among these results, the formation of chimera states characterized by the coexistence of synchronous and asynchronous groups of oscillators occupy a special position. At present, such nontrivial states remain attractive and intriguing effects for many researchers specializing in nonlinear dynamics (see recent reviews [24–29]). This interest is due to the fact that chimeras are formed because of the fundamental symmetry breaking phenomenon [30] manifested in certain populations in that in spite of the fact a homogeneous fully synchronous state exists and is stable, the system (for a number of initial conditions) can pass during the long-term evolution to a completely different (more complex) regime of its dynamics, in which apart from the groups with mutually synchronous elements, there exists a substantial part of asynchronous oscillators.

Nontrivial states in media consisting of phase oscillators with a nonlocal coupling can be described as stationary structures with spatially nonuniform complex order parameter profile that is determined locally as a measure of coherence of the mesoscopic group of neighboring elements. In particular, in this context, the absolute value of such a local complex order parameter for chimera regimes in distributed ensembles and populations with a composite topology identically equals unity in the regions where adjacent oscillators are synchronous and is smaller than unity in regions with an asynchronous behavior of elements [24–28, 31–35].

In the investigations in this field, systems consisting of nonidentical oscillators occupy a special place [13, 18, 20–23, 36–43]. In such systems, each oscillator possesses its own frequency, the value of which depends on the properties of a given element. In an ensemble consisting of a large number of oscillators, it is quite natural to assume that these frequencies are selected at random, and their distribution obeys a certain law that is formulated beforehand from physical considerations. If we consider populations with a nonlocal interaction, we can state that spatial disorder is manifested, which can significantly affect the coherence in the group of adjacent oscillators as well as the dynamics of the ensemble as a whole. On the one hand, its presence complicates analysis of the long-term behavior and the states of the medium, which are ultimately stabilized, because additional parameter responsible for the spread of frequencies appear. One can expect the emergence of some new more complex regimes that are absent in the case of identical oscillators. The degree of spatial disorder determines the bifurcation values of other quantities, at which possible scenarios of long-term evolution change qualitatively. On the other hand, there appears the possibility of an advance in the analytic description of the results of numerical simulation. This is primarily due to the fact that a fully coherent regime cannot be realized in such systems. Therefore, the degenerate situation in which the modulus of the local complex order parameter identically equals unity becomes impossible.

Distributed systems consisting of nonidentical nonlocally coupled oscillators have been actively investigated from different points of view. From a large number of publications appearing during the last decade in this field, we consider here only several key works [37–43]. In particular, in [37, 38], the long-lived states characterized by the existence of regions with different degrees of particle coherence are described. Such states are analogs of chimeras and are transformed into them in the limit of zero frequency spread. In the same publications, it was demonstrated for the first time that the Ott–Antonsen reduction [20–22], which makes it possible to obtain self-consistent dynamic equations for macroscopic complex fields (one of which being the local order parameter), can effectively be used for analyzing these regimes. A generalized phase model that can be used for describing networks of nonlocally interacting elements with different individual characteristics was considered in [39]. The key feature of the system considered in [39] is the existence of a time lag in the coupling between two pairs of elements, which is chosen at random and introduces additional disorder. In particular, it was shown that if the values of control parameters are close to critical values at which a homogeneous partially synchronous state loses its stability, the population of nonidentical phase oscillators with a time lag is transformed during its evolution into transient states distinguished by the existence of several (two or more) extrema in the distribution of averaged quantities; this in turn indicates that the medium splits into irregular (in time) alternating (in space) regions with elevated and lower coherence. In [44, 45] (in the case when the medium consists of identical particles; see, for example, [40, 41, 46]), another possible typical regime that can be reached by an oscillator ensemble has been analyzed. It will be referred below as the twisted state because it is distinguished by the fact that the mean phase at an arbitrary instant increases by $2\pi q$ upon the path-tracing of the system closed into a ring, where q is an integer. In [42], the attention of the authors was concentrated on states with irregular (chaotic) behavior of macroscopic fields. Among other things, an attempt was made at the classification of the observed turbulent regimes. In the recent publication [43], the existence of breather quasi-chimera regimes characterized, on the one hand, by a periodic time variation of the amplitude of complex mesoscopic fields at each point of space and, on the other hand, by the coexistence of regions with elevated and lower coherence was considered. It should be noted that such regimes were discovered earlier for systems of identical phase oscillators (see, for example, [32, 33]). In addition, it should be specially emphasized that in most of the aforementioned publications, either functions with a finite number of terms in the corresponding Fourier series, or rectangular finite-width distributions were used as the kernels of the integral operator describing the nonlocal interaction.

In this study, apart from the description of original results for kernels with exponentially decreasing tails, an attempt is also made at a certain systematization and generalization of the data obtained earlier and information found in the literature. We analyze synchronous and asynchronous regimes and the corresponding spatiotemporal structures in an ensemble of weakly nonidentical nonlocally coupled phase oscillators distributed uniformly over the ring. In theoretical analysis, we are using the Ott–Antonsen approach [20–22]. The form of the interaction (of the exponential type) in the medium makes it possible to pass from the integro-differential equation for the order parameter to a self-consistent system of partial differential equations for two complex fields analogously to the procedure used in [31–33]. The nonidentity of elements of the medium is a key feature that makes it possible to advance primarily in the study of the variety of stationary nonuniform local order parameter profiles and their stability as compared to those in our earlier investigations of systems of identical oscillators [31–33, 46] because the complex fields we are interested in are smooth functions modulo smaller than unity. Numerical simulation is performed using the initial model of a population consisting of a large number of phase oscillators with natural frequencies chosen at random in accordance with the Lorentz distribution, as well as on the basis of closed self-consistent equations for macroscopic (averaged) quantities.

The mathematical formulation of the problem under investigation is given in Section 2. The simplest solutions with the constant absolute value of the order parameter are described in Section 3. Here, asynchronous and partially synchronous uniform regimes, as well as twisted states, are considered. In Section 4, first, basic information and relations underlying the proposed method of the search for stationary (uniformly rotating) nonhomogeneous solution to the Ott–Antonsen equations with periodic boundary conditions are given. Then the key aspects of linear analysis of stability of the given nontrivial spatial structures that can be put in correspondence with quasi-chimera static states of the initial phase model are described. Further, the main aspects and advantages of the procedure for constructing the families of such transformations with different numbers of regions with elevated and lowered coherence are considered, and the results obtained with such an approach are formulated. In addition, the drawn conclusions are supported by direct numerical simulation of the dynamics of distributed phases and the local complex order parameter. The classes of possible observable regimes with a more complex (periodic or irregular)) behavior (in space and time) of mesoscopic (averaged) fields are considered in Section 5. The results of this study are formulated in Conclusions.

2. MODEL

Let us consider an ensemble of N nonlocally coupled nonidentical oscillators ($n = 1, 2, \ldots, N$) distributed uniformly over a segment of length L with periodic boundary conditions [37–39, 41–43]. We describe this system using the phase approximation with dynamic variables $\varphi_n(t)$, the time variation of each such variable being determined by equation

$$\frac{d\phi_n}{dt} = \omega_n + \mathrm{Im}(H_n(t)e^{-i\phi_n(t)}), \tag{1}$$

where ω_n ($n = 1, 2, \ldots, N$) are natural frequencies of the oscillators. As in most publications [18, 37–39, 41–43], we assume that quantities ω_n are chosen at random and described by the Lorentz (or Cauchy) distribution function

$$\pi g(\omega) = \frac{\gamma}{(\omega - \omega_0)^2 + \gamma^2} \tag{2}$$

with mean value ω_0 and half-width γ.

Field $H_n(t)$ acting on the oscillators has phase shift α, which is the same for all elements, and is defined in terms of the discrete convolution operator:

$$H_n(t) = e^{-i\alpha}\frac{L}{N}\sum_{\tilde{n}=1}^{N} G\left(\frac{L}{N}(n - \tilde{n})\right)e^{i\phi_{\tilde{n}}(t)}. \tag{3}$$

Its kernel $G(x)$ characterizes the interaction in the medium in question and satisfies the unit normalization condition. For $G(x)$, we choose function

$$G(x) = \kappa\cosh(\kappa(|x| - L/2))/2\sinh(\kappa L/2), \tag{4}$$

that successfully approximates the case with weak nonlocal coupling [31–33, 46]. This function adequately describes the effects associated with the influence of not only the nearest neighbors on an arbitrarily chosen element, but also of other (more remote) oscillators. We can naturally assume that this influence decreases relatively rapidly with increasing distance between particles. It should be emphasized that expression (4) in the limit $\kappa L \to +\infty$ is transformed into exponential kernel

$$G_{KB}(x) = \kappa\exp(-\kappa|x|/2)$$

from the classical work by Kuramoto and Battogtokh [47]. In fact, both $G_{KB}(x)$ and $G(x)$ in form (4) are the Green functions of the nonhomogeneous Helmholtz equation with a source on the right-hand side. However, in the former case, the system is assumed to be distributed over the entire (infinite) interval from $-\infty$ to $+\infty$, while in the latter case, the situation corresponds to a finite-length medium closed into a ring; i.e., the system satisfies periodic boundary conditions.

Several more remarks that make it possible to reduce the number of parameters in the given system are due. For example, the combination of relations (3) and (4) is invariant to scale transformations. For this reason, without loss of generality, coefficient κ can be set equal to unity. Therefore, we will henceforth assume that $\kappa = 1$, and the force of coupling between elements is determined in fact by length L of the medium. In addition, passing to the coordinate system rotating with velocity ω_0, we can easily exclude quantity ω_0 from the control parameters. Consequently, even at the stage of formulation of the problem, it is expedient to set the value of ω_0 equal to zero (i.e., we will assume below that $\omega_0 = 0$). Thus, for typical regimes of the long-term evolution of the given ensemble of nonlocally interacting oscillators, three quantities L, γ, and α are determining parameters. It should also be noted that the case of identical oscillators ($\gamma = 0$) has already been considered in our earlier publications [31–33, 46].

The model formulated above, which consists of finite number N of oscillators and described by Eqs. (1)–(4), has a wide spectrum of applications in various fields of science and technology [11, 12, 15]. However, analysis of dynamic properties and structural features of the given system in the thermodynamic limit, where we assume that it contains an infinitely large number of elements (i.e., $N \to \infty$) is often useful and even necessary in most cases for deeper understanding of the results of calculations. In this case, a transition is made from Eqs. (1) and (3) to their continuos form:

$$\frac{\partial \phi(x,t)}{\partial t} = \omega + \mathrm{Im}(H(x,t)e^{-i\phi(x,t)}), \tag{5}$$

$$H(x,t) = e^{-i\alpha}\int_0^L G(x-\tilde{x})e^{i\phi(\tilde{x},t)}d\tilde{x}. \tag{6}$$

According to our assumption, in full agreement with the initial discrete model, quantity ω at each point x of the interval from 0 to L is specified independently and randomly using probability distribution (2). It should also be noted that the integral in representation (6) of complex field $H(x, t)$ responsible for the nonlocal interaction should be treated as the limit of Lebesgue integral sums [48]. Therefore, the smoothness of function $\varphi(x, t)$ in spatial coordinate x in expressions (5) and (6) is not required. This feature of the absence of smoothness is observed in all regimes of behavior of a medium of phase oscillators considered here, which considerably complicates their analysis and classification on the microscopic level, which is limited only to relations (1)–(6). However, a transition to mesoscopic fields in the limit $N \to \infty$ makes it possible to advance significantly in the solution of this problem. The main stages of such a transition can be described as follows.

On the one hand, using the averaging procedure (see, for example, [19–22, 26]), we can determine local order parameter $Z(x, t) = \langle e^{i\phi}\rangle_{\mathrm{loc}}$, which is a continuous complex function of coordinate x and time t and satisfies inequality $|Z(x, t)| \le 1$. In the case when $|Z(x, t)| = 1$, all oscillators located near point x are synchronous in phase. If condition $0 < |Z(x, t)| < 1$ is satisfied, it is assumed that a partial synchronization regime is observed. In this case, correlations are observed in the motion of particles. Equality $|Z(x, t)| = 0$ indicates that the elements of the ensemble rotate fully asynchronously. Therefore, analogously to systems with a global interaction, complex order parameter $Z(x, t)$ plays an important role in analysis of systems with a nonlocal coupling because its amplitude characterizes the degree of local synchronization in the population, and the phase gives idea on the mean value, around which quantity φ is spread in the vicinity of the point with coordinate x.

On the other hand, the key aspects of the evolution of the oscillator medium in the phase model considered here in the thermodynamic limit can be described by introducing probability density $\rho(\varphi, \omega, x, t)$ of the distribution of dynamic variable φ for a given ω and for certain x and t. In particular, $Z(x, t)$ can obviously be defined directly using $\rho(\varphi, \omega, x, t)$ as

$$Z(x,t) = \int_{-\infty}^{+\infty}\int_{-\pi}^{+\pi} \rho(\varphi,\omega,x,t)e^{i\varphi(x,t)}d\phi d\omega. \tag{7}$$

In turn, real-valued function $\rho(\varphi, \omega, x, t)$ must satisfy continuity equation

$$\frac{\partial\rho}{\partial t} + \frac{\partial}{\partial\varphi}(\omega\rho + \mathrm{Im}(He^{-i\varphi})\rho) = 0. \tag{8}$$

In [20, 21], an attracting manifold was found for this equation with $H = H(t)$. Later, the approach developed in [20, 21] and the results obtained there were generalized to the case when field H acting on the elements of the ensemble depends not only on time t, but also on spatial coordinate x; i.e., $H = H(x, t)$ in such a situation (see, for example, the literature cited in [22, 37] and review [26]). Here, we will consider only briefly the main idea of this method and its consequences.

Considering that the natural frequencies of the phase oscillators in Eqs. (1) and (5) are chosen independently and taking into account cyclicity condition $\rho(\varphi, \omega, x, t) = \rho(\varphi + 2\pi, \omega, x, t)$, it is expedient to seek the solution to Eq. (8) in the form of expansion

$$\rho(\varphi,\omega,x,t) = \frac{g(\omega)}{2\pi}\left(1 + \sum_{m=1}^{+\infty}[a_m(\omega,x,t)e^{im\varphi} + \mathrm{C.c.}]\right), \tag{9}$$

which is in fact a Fourier series in dynamic variable φ. For the Ott–Antonsen manifold we are interested in (after the names of the authors of articles [20, 21]), all coefficients $a_m(\omega, x, t)$ with subscripts $m > 1$ in spectral representation (9) can be expressed in terms of factor

$a_1(\omega, x, t)$ of the first harmonic by raising it to the corresponding power:

$$a_m(\omega, x, t) = a_1^m(\omega, x, t). \tag{10}$$

In this case, the behavior of $a_1(\omega, x, t)$ is described by equation

$$\frac{\partial a_1}{\partial t} = -i\omega a_1 + \frac{1}{2}(H^* - Ha_1^2), \tag{11}$$

which can easily be verified by substituting expression (9) together with (10) directly into (8).

Further, following the general conception proposed in [20, 21] (see also [22, 26, 37]) and using expansion (9) in equality (7), we can easily establish the relation between $a_1(\omega, x, t)$ and $Z(x, t)$, from which, after the imposition of the above assumption that function $g(\omega)$ has the form of Cauchy distribution (2) and the integration over ω, it follows that $Z(x, t) = a_1^*(-i\gamma, x, t)$ in the given situation. It should be noted that we assumed here that $\omega_0 = 0$. Proceeding from Eq. (11), we obtain the following integro-differential equation for order parameter $Z(x, t)$:

$$\frac{\partial Z}{\partial t} = -\gamma Z + \frac{1}{2}(H - H^* Z^2), \tag{12}$$

where $H(x, t)$ is now expressed directly in terms of $Z(x, t)$ with the help of convolution operator

$$H(x,t) = e^{-i\alpha}\int_0^L G(x - \tilde{x})Z(\tilde{x},t)d\tilde{x}, \tag{13}$$

and the integral over the space in this equation should be treated in the Riemann sense (in contrast to relation (6)). In addition, for the Ott–Antonsen manifold with allowance for relation (2) in $Z(x, t)$, we can reconstruct probability density $f(\varphi, x, t)$ of the spread of φ for certain x and t [37, 38],

$$\begin{aligned} f(\varphi, x, t) &= \int_{-\infty}^{+\infty} \rho(\varphi, \omega, x, t) d\omega \\ &= \begin{cases} \delta(\varphi - \arg(Z)), & |Z| = 1, \\ (1 - |Z|^2)/2\pi(1 - 2|Z|\cos(\varphi - \arg(Z)) + |Z|^2), & |Z| < 1, \end{cases} \end{aligned} \tag{14}$$

(here we appled the expression for the sum of a trigonometric progression). This means that profile $Z(x, t)$ can be put in correspondence to phase distribution $\varphi(x, t)$ (and, naturally, vice versa) at any preset instant.

All circumstances listed above render the methods based on the ideas developed in [20–22] mainly for analyzing the behavior of mesoscopic fields $Z(x, t)$ and $H(x, t)$ a quite effective tool for studying and predicting possible key regimes of the behavior of many-particle model (1)–(4) we are interested in. In further analysis, we take one more step for simplifying the investigation of the spatial structure of $Z(x, t)$ and $H(x, t)$. Using specific form (4) for kernel $G(x)$, we can easily pass from relation (13) to an equivalent differential equation

$$\frac{\partial^2 H}{\partial x^2} - H = -Ze^{-i\alpha} \tag{15}$$

with periodic boundary conditions $[0, L)$, namely,

$$\begin{gathered} H(0,t) = H(L,t), \\ \frac{\partial H}{\partial x}(0,t) = \frac{\partial H}{\partial x}(L,t) = 0. \end{gathered} \tag{16}$$

In this way, we have constructed for initial problem (1)–(4) in the limit $N \to \infty$ a reduction involving a transition from analysis of nonsmooth phase profiles to operation with continuous (on characteristic scales of the medium) distributions $Z(x, t)$ and $H(x, t)$. It will be shown below that for deeper understanding of processes in collective effects occurring in system (1)–(4) with large number N of elements, it is expedient to analyze the dynamics of an ensemble of phase oscillators and the evolution of complex local order parameter $Z(x, t)$ specified by system (12), (15) of partial differential equations with boundary conditions (16).

Before passing to a consistent and detail description, we will briefly consider the typical regimes of the behavior of a closed circular system of nonlocally interacting elements, which are established in numerical calculations. Analysis based on model (1)–(4) and performed using the simulation of self-consistent equations (12), (15) has proved the existence of the following stable structurally different states:

(1) fully asynchronous state (Figs. 1a and 1b);

(2) homogeneous partially synchronous state (Figs. 1c and 1d);

(3) partially synchronous state with a gradient phase distribution (Figs. 1e and 1f);

(4) spatially inhomogeneous cluster partially synchronous state (Figs. 1g and 1h) in which several (most often, static) regions with a higher or lower degree of coherence of the oscillators can be singled out explicitly;

(5) breather cluster regime, in which several synchronous clusters with different mean frequencies coexist (Fig. 1i, 1j);

(6) intermittency regime, in which the intervals with irregular dynamics of averaged fields on the spatiotemporal diagram change to extended intervals with their regular behavior (which can be treated as cluster synchronization regions; Figs. 1k and 1l);

(7) turbulence regime with a complex irregular behavior of mesoscopic characteristics of the system, when it is impossible to single out extended time intervals during which a quasi-static structure of spatial regions with different degrees of coherence is observed (Figs. 1m and 1n).

It should be noted that the second and third types of states in the limit of infinitely small spread in natural frequencies ($\gamma \to 0$) are transformed into fully syn-

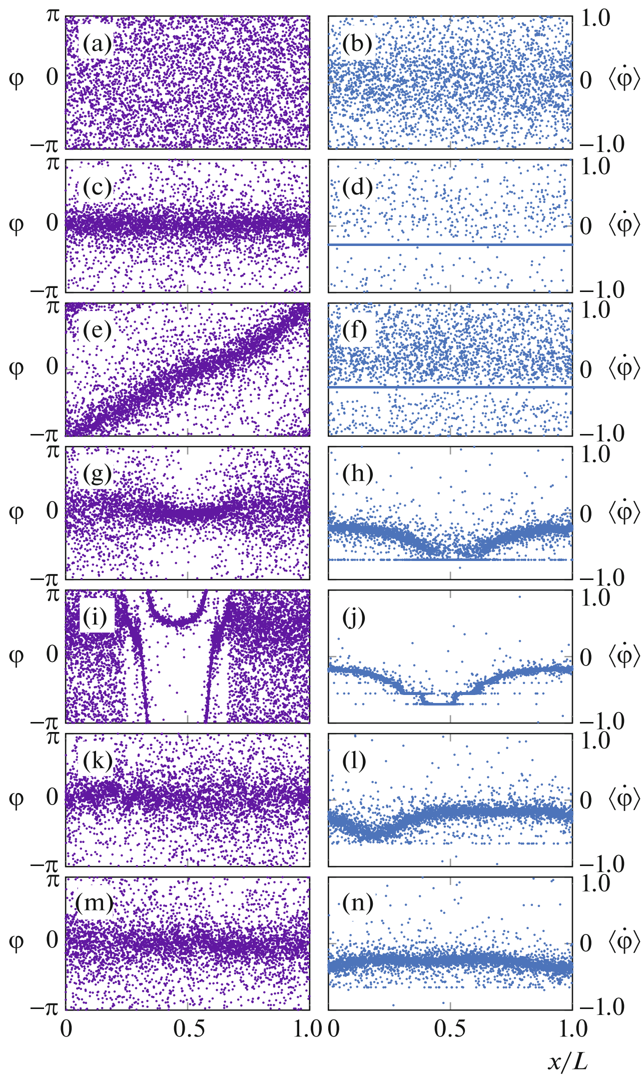

Fig. 1. Regimes realized in system (1)–(4). Left panels: snap shots of phases φ_n. Right panels: average frequencies $\langle\dot{\varphi}_n\rangle$ of oscillators. (a, b) Fully asynchronous state for $\alpha = 0.2$, $\gamma = 0.5$, $L = 5.0$. (c, d) Homogeneous partially synchronous regime for $\alpha = 0.4$, $\gamma = 0.25$, $L = 6.0$. (e, f) Partially synchronous twisted state for $\alpha = 0.4$, $\gamma = 0.25$, $L = 25.0$. (g, h) Regime of cluster synchronization for $\alpha = 1.457$, $\gamma = 0.02$, $L = 6.0$. (i, j) Breather cluster regime for $\alpha = 1.457$, $\gamma = 0.002$, $L = 7.005$. (k, l) Intermittence regime for $\alpha = 1.457$, $\gamma = 0.02$, $L = 8.837$. (m, n) Turbulent regime for $\alpha = 1.457$, $\gamma = 0.02$, $L = 16.655$.

chronous states, while the formations described in items (4) and (5) in the case of identical particles are transformed into stationary and breather chimeras [26, 31–34]. It should be also emphasized that Fig. 1 does not fully reflect all features of the last two of the listed regimes. It can easily be noted, however, that the phase coherence level for such states of the ensemble with finite number N of elements varies with time in the vicinity of each spatial point, and synchronous clusters consisting of macroscopic number of oscillators cannot be singled out in the average frequency distribution.

To understand and explain the peculiarities and conditions for stabilization of each regime observed in direct simulation of system (1)—(4), we will adopt the following strategy. Above all, we will try to find the corresponding solutions to the Ott–Antonsen equation (12), (15) with boundary conditions (16) in the thermodynamic limit and to test their stability; then we will verify the obtained analytic results numerically using initial model (1)–(4).

3. STATES WITH A UNIFORM IN SPACE DEGREE OF PHASE SYNCHRONIZATION OF NEIGHBORING OSCILLATORS

3.1. Homogeneous States

Let us begin our analysis with the simplest class of solutions to self-consistent system of equations (12), (15) with boundary conditions (16). We are speaking of time-independent homogeneous solutions for which the modulus of local complex order parameter $Z(x, t)$ is a constant quantity, and the phase increases with time linearly and is independent of spatial coordinate x. In the initial model (1)–(4), a uniform (on the average) rotation of a significant group of oscillators is observed, and the degree of coherence of elements at each point is the same. In this case, we seek functions $Z(x, t)$ and $H(x, t)$ in form

$$Z(x,t) = z_0 e^{i\Omega t}, \quad H(x,t) = h_0 e^{i\Omega t}, \tag{17}$$

where z_0 and h_0 denote constant (in accordance with our assumption) amplitudes of averaged fields; Ω (here and in different situations below) plays the role of the parameter that determines their common observed frequency. Substituting relation (17) into (12) and (15), we obtain the following relation between z_0, h_0, and Ω:

$$2z_0(i\Omega + \gamma) = z_0(h_0 - h_0^* z_0^2), \quad h_0 = z_0 e^{-i\alpha}. \tag{18}$$

It should be noted above all that if $z_0 = h_0 = z_{as} = 0$, algebraic equalities (18) obviously hold for any α and γ irrespective of length L of the medium. In addition, quantity Ω remains indeterminate, i.e., there is certain arbitrariness in its choice (we can also set $\Omega = 0$). Such a trivial solution to Ott–Antonsen equations (12), (15) corresponds to fully asynchronous behavior of elements in the given ensemble, when the phases of the oscillators are distributed uniformly in the interval from $-\pi$ to π at each instant.

However, we are interested primarily in steady-state regimes for which the mesoscopic characteristics of the distributed population have finite values, indicating the existence of correlations in the motion of adjacent elements. Relations (18) directly imply that such partially synchronous states can be determined using the class of time-independent homogeneous solutions considered here. Such collective modes exist when control parameters α and γ satisfy condition $2\gamma < \cos\alpha$ (since γ is the half-width of the natural frequency distribution, we have $\gamma \geq 0$). In this case, we can easily verify that equalities (18) can be satisfied if

$$|z_0|^2 = r_{\text{hps}}^2 = 1 - 2\gamma/\cos\alpha,\\ \Omega_{\text{hps}} = \gamma\tan\alpha - \sin\alpha. \tag{19}$$

It should be emphasized that these relations hold when requirement $|z_0| \leq 1$ that follows from the definition of the local order parameter is met. It should also be noted that in accordance with relations (19), length L of the system does not affect the existence of uniform partially coherent regimes. In spite of the fact that the results of numerical simulation are in conformity in many respects with the conclusions drawn as a result of the above analysis (in particular, the synchronization level calculated using the calculations based on model (1)–(4) coincides to a high degree of accuracy with estimate (19)) for a number of situations in which, for example, phase detuning α is close to $\pi/2$ ($\alpha \lesssim \pi/2$) and γ is slightly smaller than $\cos\alpha/2$ ($\gamma \lesssim \cos\alpha/2$), the homogeneous partially synchronous states stop being observed starting from a certain value of L. We will explain below the behavior of initial system (1)–(4) and formulate the reasons for it based on the linear analysis of stability of time-independent solutions (19) to Ott–Antonsen equations (12), (15), but before that, we consider one more class of regimes for which the coherence level of the oscillators turns out to be the same over the entire medium.

3.2. Twisted States

In the case of identical oscillators, when $\gamma = 0$, the homogeneous partially coherent states considered in the previous section are transformed into fully synchronous states for which $|Z(x, t)| = 1$ for any x at any instant t, which follows directly from relations (19) in the limit $\gamma \to 0$. However, one more regime with $|Z(x, t)| = 1$ at all sites exists for a spatially distributed ensemble consisting of nonlocally interacting particles with identical individual characteristics. A distinguishing feature for this regime is the existence of a constant phase difference upon a transition from one point to another (for an arbitrarily chosen n, equality $\varphi_{n+1}(t) - \varphi_n(t) = \Delta\varphi = \text{const} \neq 0$ holds) so that the total phase shift differs from zero during the passage over the entire medium. Such a state is referred to as the splay state [40, 44, 45]. We can naturally expect the existence of analogs of these states for $\gamma \neq 0$ for model (1)–(4) under investigation. As a result of the random spread in the natural frequencies of the oscillators, the phase distribution will obviously also become irregular. However, despite of the apparent disorder the degree of which depends on γ, the behavior of mesoscopic fields remains the same as for $\gamma = 0$, and the general tendencies (primarily, the slope) in the $\varphi(x, t)$ (or $\varphi_n(t)$) profile are preserved. It should be noted that attempts at analysis of such states were made earlier, but for other forms of kernel $G(x)$ (see, for example, [40, 41, 44, 45]).

Considering that twisted regimes, as well as homogeneous states considered above, are characterized by a constant value of the modulus of local order parameter $Z(x, t)$ over the entire length of the medium, we will seek fields $Z(x, t)$ and $H(x, t)$ in the form analogous to (17):

$$Z(x,t) = z_0 e^{i\Omega t - iQx}, \quad H(x,t) = h_0 e^{i\Omega t - iQx}, \tag{20}$$

the only difference being that the exponent in these expressions acquires an additional term proportional to spatial coordinate x and responsible for the common slope of the phase front of functions $Z(x, t)$ and $H(x, t)$. In view of the periodicity of the boundary conditions, coefficient Q in such a linear dependence must be defined as $Q = 2\pi q/L$, where integer $q = \pm 1, \pm 2, \ldots$ (that differs from zero in the situation of interest to us here) indicates the number of revolutions through 2π made by the averaged phase upon the full path-tracing of the system. Substituting relations (20) into Ott–Antonsen equations (12), (15), we obtain two algebraic equalities

$$2(i\Omega + \gamma)z_0 = h_0 - h_0^* z_0^2, \quad (1 + Q^2)h_0 = z_0 e^{-i\alpha}, \tag{21}$$

for which we can easily find nontrivial solution

$$|z_0|^2 = r_{\text{gps}}^2 = 1 - \frac{2\gamma(1 + Q^2)}{\cos\alpha},\\ \Omega_{\text{gps}} = \gamma\tan\alpha - \frac{\sin\alpha}{1 + Q^2}, \tag{22}$$

corresponding to twisted states. These expressions imply directly that such regimes exist only if $\cos\alpha > 2\gamma$. In addition, requirement $r_{\text{gps}}^2 > 0$ leads to the condition for length L of the distributed population of phase oscillators. In accordance with this condition, the twisted states with number of revolutions q exist only when size L of an ensemble closed into a ring exceeds critical value $L_{\text{gps}}(q)$; i.e.

$$L > L_{\text{gps}}(q) = 2\pi q\sqrt{2\gamma/(\cos\alpha - 2\gamma)}. \tag{23}$$

It should be noted that if we formally set $q = 0$ in expressions (22), these expressions coincide with (19). This is another confirmation of the interrelation between partially synchronous homogeneous and twisted states. However, it is still expedient to distinguish between the two different classes of such regimes. In particular, this point of view is supported by the global order parameter $R(t)$ that is an important characteristic in the synchronization theory,

$$R(t) = \left|\frac{1}{N}\sum_{n=1}^{N} e^{i\varphi_n}\right|, \tag{24}$$

which can be calculated in limit $N \to \infty$ using formula

$$R(t) = \left|\frac{1}{L}\int_0^L Z(\tilde{x}, t)d\tilde{x}\right|. \tag{25}$$

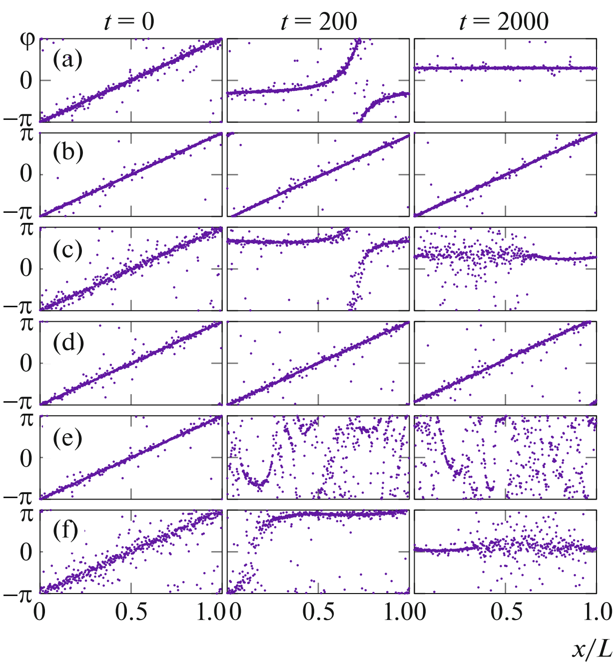

Fig. 2. Evolution of the twisted partially synchronous state (TS). Results of direct numerical simulation of system (1)–(4) for $\alpha = 1.457$. Snap shots of phases φ_n for regions represented in Fig. 3. Region A: (a) unstable TS evolving to the homogeneous regime with $|z| = r_{\text{hps}}$ for $\gamma = 0.001$, $L = 4$; (b) stable TS for $\gamma = 0.001$, $L = 14$; region B: (c) unstable TS evolving to the nonuniform regime for $\gamma = 0.003$, $L = 4$; (d) stable TS for $\gamma = 0.003$, $L = 12$; (e) unstable TS evolving to the turbulent regime for $\gamma = 0.003$, $L = 28$; region C: (f) unstable TS evolving to inhomogeneous regime for $\gamma = 0.005$, $L = 4$.

For homogeneous partially synchronous states, this parameter takes finite values, while for twisted regimes, it is always zero, which can easily be verified using relations (20). It should also be emphasized that for fixed α and γ, the degree of local coherence in the former case is always higher than in latter case.

Numerical calculations performed using initial model (1)–(4) demonstrate good agreement with the above description for certain selected values of α and γ. First, this is manifested in that partially synchronous twisted states are observed for long time intervals and remain insensible to small perturbations, i.e., are possible stable versions of rotation of phase oscillators (see Fig. 1e and Fig. 2). Second, the degree of local coherence, which is determined by the absolute value of the complex order parameter calculated using mesoscopic averaging of the results of direct simulation, is reproduced quite adequately by formula (22). In addition, the precision of estimate (22) increases with number N of elements in the system. However, in numerical calculations, twisted states can be realized not for all $L > L_{\text{gps}}(q)$. For example, Figs. 2a and 2b illustrate two situations corresponding to the same choice of α and γ ($\alpha = 1.457$ and $\gamma = 0.001$), but to different values of $L > L_{\text{gps}} \approx 0.841$ ($L = 4$, Fig. 2a, and $L = 14$, Fig. 2b). It can be seen that for $L = 4$ (see Fig. 2a), the state with $q = 1$ number of revolutions of average phase through 2π decays relatively rapidly and is transformed into a partially synchronous uniform regime. However, when $L = 14$ (see Fig. 2b), no such process occurs, and the characteristic features of the spatial distribution of dynamic variables $\varphi_n(t)$ do not noticeably change over infinitely long time intervals. In spite of the fact that size L of the system satisfies the existence condition (23), an analogous effect of twisted state breaking is observed for $\alpha = 1.457$ and $\gamma = 0.003$ (Figs. 2c, 2d, and 2e). It should be noted, however, that in contrast to the case with $\alpha = 1.457$ and $\gamma = 0.001$, the breaking of the phase profile formed in accordance with relations (20), (22), and (14) occurs in relatively short ($L = 4$, see Fig. 2c) as well as in extended populations ($L = 28$, see Fig. 2e), and twisted states are stable only in a certain interval of lengths L. To explain the features of evolution of the regimes theoretically observable in numerical calculations, linear analysis of their stability is required.

3.3. Stability of Partially Synchronously Homogeneous and Twisted States

In this section, we perform the linear analysis of stability of the above regimes of the behavior of a system of nonlocally coupled nonidentical phase oscillators in the thermodynamic limit based on the Ott–Antonsen reduction. This will allow us to remove the aforementioned apparent (but actually nonexisting) contradictions between the developed theoretical description and numerical calculations. We will carry out such analysis within a unified formalism that is general and can be used for homogeneous as well as twisted states. Note that for convenience and better visualization, we will employ the equivalence of Eq. (15) with periodic boundary conditions (16) to the convolution operator with kernel (13).

To test analytically the stability of temporal distributions of oscillators considered here, we represent complex fields $Z(x, t)$ and $H(x, t)$ in form

$$\begin{aligned} Z(x,t) &= (z_0 + \mathcal{Z}(x,t))e^{i\Omega t - iQx}, \\ H(x,t) &= (h_0 + \mathcal{H}(x,t))e^{i\Omega t - iQx}. \end{aligned} \tag{26}$$

Here, we have taken into account explicitly the key features of phase profiles of interest to us, which correspond (for fixed length L of the medium) to the time-independent solutions to Ott–Antonsen equations (12), (15), characterized by parameters Ω and Q. In expressions (26), functions $\mathcal{Z}(x, t)$ and $\mathcal{H}(x, t)$ play the role of weak (and periodic in spatial coordinate x) perturbations to homogeneous state with $Q = 0$ and to the twisted solution with $Q \neq 0$. Substituting relations (26) into (12) and (13) and linearizing them in the vicinity of z_0 and h_0 with allowance for smallness of $\mathcal{Z}(x, t)$ and $\mathcal{H}(x, t)$, we obtain the following linear integro-differential equation with coefficients independent of x and t:

$$\frac{\partial\mathcal{Z}}{\partial t} = -\left(\gamma + i\Omega + \frac{e^{i\alpha}|z_0|^2}{1+Q^2}\right)\mathcal{Z} + \frac{1}{2}(\mathcal{H} - |z_0|^2\mathcal{H}^*), \quad (27)$$

$$\mathcal{H}(x,t) = e^{-i\alpha}\int_0^L G(x-\tilde{x})e^{iQ(x-\tilde{x})}\mathcal{Z}(\tilde{x},t)d\tilde{x}. \quad (28)$$

Further, following one of the versions of the standard procedure of stability test for spatiotemporal structures, we will seek $\mathcal{Z}(x, t)$ as a superposition of two orthogonal components written in factorized form:

$$\mathcal{Z}(x,t) = \mathcal{A}(x)e^{\Lambda t} + \mathcal{B}^*(x)e^{\Lambda^* t}, \quad (29)$$

where complex number Λ, which has both real and imaginary parts in the general case, fully characterizes the dynamics of each term in sum (29). Under the assumption that the system considered here is closed into a ring (i.e., periodic boundary conditions are satisfies at the ends of segment $[0, L)$), because of the constancy of factors in all terms with $\mathcal{Z}$ and $\mathcal{H}$ in relation (29), we can choose functions proportional to e^{iKx} for $\mathcal{A}(x)$ and $\mathcal{B}(x)$:

$$\mathcal{A}(x) = ae^{iKx}, \quad \mathcal{B}(x) = be^{iKx}, \quad (30)$$

where wavenumbers $K = 2\pi k/L$ with $k = 0, 1, 2, \ldots$ define spatial period of the mode, which does not exceed size L of the system. After the substitution of relations (29) and (30) into (27), (28), it remains for us to calculate constant complex amplitudes a and b, and the requirement of the existence of nontrivial solutions for which at least one of the amplitude differs from zero will allow us to determine the corresponding values of Λ. As a result, we obtain the problem for eigenvectors $\xi = (a, b)^T$ and eigenvalues Λ for 2×2 matrix $\hat{\mathbf{P}}$:

$$\Lambda\boldsymbol{\xi} = \hat{\mathbf{P}}\hat{\boldsymbol{\xi}}, \quad \hat{\mathbf{P}} = \begin{pmatrix} p_{11} & p_{12} \\ p_{21} & p_{22} \end{pmatrix}, \quad (31)$$

where

$$\begin{aligned} p_{11} &= -\gamma - i\Omega - \frac{e^{i\alpha}|z_0|^2}{1+Q^2} + \frac{e^{-i\alpha}}{2(1+(K-Q)^2)}, \\ p_{12} &= -\frac{e^{i\alpha}|z_0|^2}{2(1+(K+Q)^2)}, \\ p_{21} &= -\frac{e^{-i\alpha}|z_0|^2}{2(1+(K-Q)^2)}, \\ p_{22} &= -\gamma + i\Omega - \frac{e^{-i\alpha}|z_0|^2}{1+Q^2} + \frac{e^{i\alpha}}{2(1+(K+Q)^2)}. \end{aligned} \quad (32)$$

Relations (31) directly imply that for determining Λ, we must solve the quadratic equation, a pair of the roots to which can be written directly in terms of trace $\mathrm{tr}\hat{\mathbf{P}}$ and determinant $\det\hat{\mathbf{P}}$ of the just introduced matrix $\hat{\mathbf{P}}$:

$$\Lambda_{1,2} = \frac{1}{2}\left(\mathrm{tr}\hat{\mathbf{P}} \pm \sqrt{(\mathrm{tr}\hat{\mathbf{P}})^2 - 4\det\hat{\mathbf{P}}}\right). \quad (33)$$

Proceeding from this expression, we can easily draw the conclusion about the stability of regimes with a uniform distribution of the complex parameter modulus. If real part Λ_1 or Λ_2 turns out to be positive, small perturbations must increase exponentially with time in accordance with relation (29).

Based on the criterion formulated above, we can now determine the behavior of deviations of $\mathcal{Z}(x, t)$ from z_0, which correspond to one of three regimes considered above (namely, to the fully asynchronous, partially synchronous, and twisted states). The above results are summarized in Fig. 3.

The fully asynchronous regime with $|z_0| = z_{\mathrm{as}}$ attracts nearby trajectories of the system if $\cos\alpha < 2\gamma$ for any length L of the medium so that the situation without any phase correlations between individual elements is realized during the long-term evolution. In the opposite case, when $\cos\alpha > 2\gamma$, the asynchronous regime turns out to be unstable (Figs. 3a and 3b). Spatially homogeneous linear modes with $K = 0$ lead to the evolution of this instability. It should be noted that this result is universal for standard forms of kernels used for describing the nonlocal interaction between elements of the population, which completely coincides with the conclusion drawn in [41], where the dynamics of the trivial regime with $|z_0| = z_{\mathrm{as}} = 0$ for rectangular coupling function $G(x)$ is considered in detail. It should also be noted that such instability is quite common in nonlinearly distributed models and is called the Eckhaus instability after the author of monograph [49].

For partially coherent states with $Q = 0$, $|z_0| = r_{\mathrm{hps}}$ and $\Omega = \Omega_{\mathrm{hps}}$ (see formula (19)), which are formed under the same conditions in which an asynchronous regime loses its stability, we can easily analyze analogously the behavior of small perturbations $\mathcal{Z}(x, t)$ in form (29), (30). Using expressions (19), (31), (32), and (33), after a number of algebraic transformations, we obtain

$$\Lambda_{1,2} = \gamma - \cos\alpha\left(1 - \frac{I(K)}{2}\right) \pm \frac{1}{2}\sqrt{\left(I(K)\left(1 - \frac{2\gamma}{\cos\alpha}\right)\right)^2 - (2\gamma\tan\alpha - I(K)\sin\alpha)^2}, \quad (34)$$

where $I(K) = (1 + K^2)^{-1}$ is the coefficient, to the multiplication by which the convolution operator in relation (28) is reduced if we assume that $\mathcal{H}(x, t)$, as well as $\mathcal{Z}(x, t)$, is proportional to e^{iKx}. Analysis of expression (34) shows that for $\gamma < (\cos\alpha)^3$, the homogeneous partially synchronous regime is stable for any value of L. When $\gamma > (\cos\alpha)^3$, condition $\mathrm{Re}\Lambda < 0$ existing

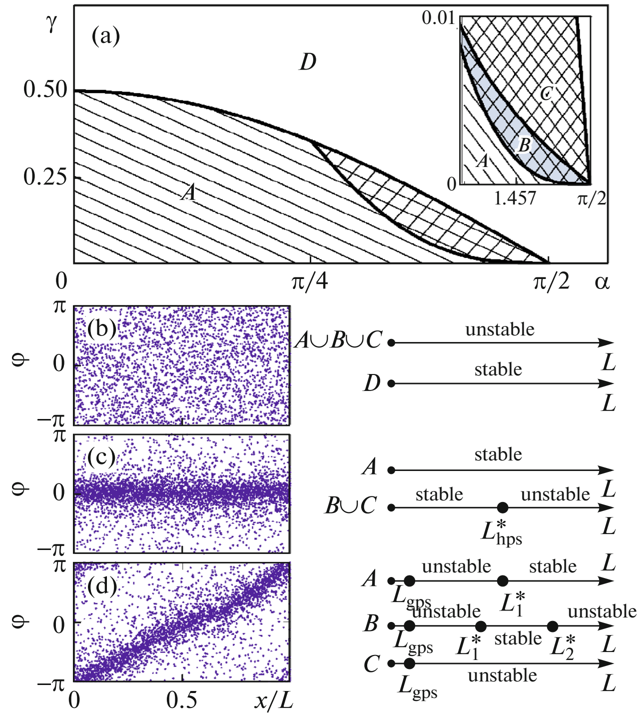

Fig. 3. (a) Regions (on the plane of parameters α and γ) of existence and stability of regimes with a uniform distribution of the synchronization level over the ensemble. For such regimes, the amplitude of local order parameter $Z(x, t)$ is the same at any point of the medium at each instant. (b) Asynchronous state exists for all α and γ irrespective of the length of the medium. It is unstable in regions A (part of the (α, γ) plane with single hatching), B (shaded region with double hatching), and C (light region with double hatching) and stable in region D (part of region α, γ without shading). (c) Homogeneous partially synchronous state exists and is stable for all values of L if the pair of quantities α and γ is chosen from region A. If, however, point α, γ lies in region B or C, there exists a critical value starting from which this regime becomes unstable. There are no such states in region D. (d) Twisted partially synchronous state exists only in regions A, B, and C when $L > L_{gps}$. This regime is stable in regions A and B if $L > L_1^*$ and $L_1^* < L < L_2^*$, respectively. In region C, the twisted state is unstable everywhere.

only for $\gamma < \cos\alpha/2$ is satisfied only if $K = 2\pi m/L$ (m = 0, 1, 2, ...) is larger than a certain critical value $K^*_{hps}(\alpha, \gamma)$. This means that there exists limiting length $L^*_{hps}(\alpha, \gamma)$, the excess over which renders the corresponding spatially homogeneous regimes of the system behavior unstable:

$$L^*_{hps} = 2\pi\sqrt{\frac{\cos^4\alpha - 2\gamma\cos^3\alpha + \gamma^2}{(\cos\alpha - 2\gamma)(\gamma - \cos^3\alpha)}}. \qquad (35)$$

As regards the twisted states each of which is determined by its own value of $Q = 2\pi q/L$ ($q = \pm1, \pm2, \ldots$) and by formulas (22) for $|z_0| = r_{gps}$ and Ω_{gps}, analysis of their stability and the corresponding results appear as slightly more complicated. For example, detailed analysis of eigenvalues $\Lambda_{1,2}$ shows that depending on the values of parameters α and γ, we can single out different situations depicted qualitatively in Fig. 3d. Figure 3a shows the boundaries of the regions corresponding to these three situations for $q = \pm1$. If we choose α and γ from the part of the plane with single hatching (region A), there exists critical length L_1^* such that for $L < L_1^*$, the twisted regime is unstable, while for $L > L_1^*$, it is stable (see Fig. 2b). This is also confirmed by direct numerical calculations based on model (1)–(4) (see, for example, Figs. 2a and 2b). For thin layer B, there are two critical values of length, L_1^* and L_2^*. In this case, the state with a phase shift of 2π is stable in interval $L_1^* < L < L_2^*$ (Fig. 2d) and unstable for $L < L_1^*$ (Fig. 2c) and $L > L_2^*$ (Fig. 2e). In region C, the twisted regime is unstable for any value of L (Fig. 2f). It should be noted that in this case, we cannot write explicit expressions for L_1^* and L_2^* and have to determine them numerically.

It should be emphasized concluding this section that the determined conditions of existence and stability of regimes with a spatially uniform degree of synchronization of phase oscillators, as well as the existence of different critical values for the length of the medium, now successfully explain the behavior of system (1)–(4), which is demonstrated in direct numerical calculations (see Fig. 2). However, less trivial states that will be considered below can also set in during the long-term evolution.

4. STATES WITH A STATIC SPATIALLY NONUNIFORM DISTRIBUTION OF THE PHASE SYNCHRONIZATION DEGREE FOR ELEMENTS IN THE ENSEMBLE

4.1. Stationary Solution to the Ott–Antonsen Equations

It was found from detailed analysis of the long-term evolution scenarios of model (1)—(4) depending on phase shift α, spatial disorder degree γ, and length L of the medium based on direct numerical simulation that cluster partially synchronous regimes of rotation (both limiting and transient), for which several static or quasi-static regions with different oscillator coherence levels can be singled out explicitly, play a special role. Examples of transitions of the studied system into such states are given in Figs. 2c and 2f, which show how the twisted distribution of phases with identical values of the local order parameter modulus is violated in interval [0, L), and the pattern with characteristic features reflected on snap shots at t = 2000 is stabilized over the entire time of further calculations. It can be seen in these fragments that there exist two regions with a higher and lower degrees of correlation of motion of adjacent elements. This suggests that the profile of each mesoscopic field introduced earlier using the averaging procedure becomes and remains spatially nonuniform. Such long-lived modes of the behavior of distributed populations are of special interest primarily for the following two reasons. First, these nontrivial regimes are observed in the ensembles of nonlocally coupled phase oscillators considered here even when the partially synchronous homogeneous state is stable. Second, for identical elements (i.e., in the limit $\gamma \to 0$), the structural formations analogous to those shown in Figs. 2c and 2f, as well as in Figs. 1g and 1i, are transformed into chimeras (in their classical sense), which are distinguished by the presence of macroscopic groups with fully synchronous rotation along with groups with partially coherent motion of elements [24–29]. These facts lead to the conclusion concerning the possibility of the fundamental effect of partial symmetry breaking in the states considered in this section [30].

To explain and describe in detail in the thermodynamic limit the key features of stationary spatial structures with regions of elevated and lowered degrees of the local phase coherence in the behavior of elements of a medium closed into a ring, we construct and analyze the (modulo) time-independent solutions to the reduced problem obtained using the Ott–Antonsen approach and formulated here in the form of a set of two partial differential equations (12) and (15) with boundary conditions (16). We write complex fields $Z(x, t)$ and $H(x, t)$ in form

$$Z(x,t) = z(x)e^{i\Omega t}, \quad H(x,t) = h(x)e^{i\Omega t}, \tag{36}$$

where Ω plays the role of the unknown parameter to be determined. Substituting expressions (36) for mesoscopic quantities $Z(x, t)$ and $H(x, t)$ into Eqs. (12) and (15), we arrive at the following system consisting of the algebraic equality and a second-order ordinary differential equation, which contain complex functions $z(x)$ and $h(x)$, which depends on variable x alone:

$$2(-i\Omega - \gamma)z + h - h^*z^2 = 0, \tag{37a}$$

$$h'' - h + ze^{-i\alpha} = 0. \tag{37b}$$

Here and below, the prime denotes the derivative with respect to coordinate x. When $\gamma \neq 0$ (i.e., the oscillators are nonidentical and differ in their individual characteristics), for $N \to \infty$, interval $[0, L)$ contains not a single point in a small neighborhood of which full phase synchronization can be achieved and, hence, the absolute value of the local order parameter is always smaller than unity (i.e., $|z(x)| < 1$). Then we can easily express using relation (37a) $h(x)$ in terms of $z(x)$:

$$h = 2\left(\frac{i\Omega}{1+|z|^2} + \frac{\gamma}{1-|z|^2}\right)z. \tag{38}$$

Let us now write $z(x)$ as

$$z(x) = r(x)e^{i\theta(x)}, \tag{39}$$

by introducing two real functions $r(x)$ and $\theta(x)$, which can naturally be referred to as the amplitude and the phase, respectively, for $z(x)$, the only difference from the classical definitions being that we assume for convenience that $r(x)$ can change sign and, in turn, $\theta(x)$ is continuous including at the points at which $r(x)$ vanishes. Then expression (38) for $h(x)$ takes form

$$h = 2re^{i\theta}\left(\frac{i\Omega}{1+r^2} + \frac{\gamma}{1-r^2}\right). \tag{40}$$

Substituting this expression into (37b) and equating to zero the real and imaginary parts of the resultant expression separately we pass to the following pair of equations:

$$\begin{aligned}&\frac{\gamma(1+r^2)}{(1-r^2)^2}r'' - \frac{\Omega r}{1+r^2}\theta'' - \frac{2\Omega(1-r^2)}{(1+r^2)^2}r'\theta' \\ &\quad + \frac{2\gamma r(r^2+3)}{(1-r^2)^3}(r')^2 - \frac{\gamma r}{1-r^2}(\theta')^2 \\ &\quad = \frac{\gamma r}{1-r^2} - \frac{r}{2}\cos\alpha,\end{aligned} \tag{41a}$$

$$\begin{aligned}&\frac{\Omega(1-r^2)}{(1+r^2)^2}r'' - \frac{\gamma r}{1-r^2}\theta'' + \frac{2\gamma(1+r^2)}{(1-r^2)^2}r'\theta' \\ &\quad + \frac{2\Omega r(r^2-3)}{(1+r^2)^3}(r')^2 - \frac{\Omega r}{1+r^2}(\theta')^2 \\ &\quad = \frac{\Omega r}{1+r^2} + \frac{r}{2}\sin\alpha,\end{aligned} \tag{41b}$$

which can be reduced by introducing new variable $u = r'$ and performing additional substitution $v = r^2\theta'$ and a number of transformations to the following third-order ordinary differential equations for $r(x)$, $u(x)$, and $v(x)$ with free parameter Ω for preset values of α and γ:

$$r' = u, \tag{42a}$$

$$\begin{aligned}u' &= \frac{1}{2(\gamma^2(1+r^2)^4 + \Omega^2(1-r^2)^4)(1-r^4)r^3} \\ &\times(-4r^4u^2(\gamma^2(r^2+3)(1+r^2)^4 + \Omega^2(r^2-3)(1-r^2)^4) \\ &- 2(8\gamma\Omega vur^3 + \gamma^2(v^2+r^4)(1+r^2)^2 \\ &+ \Omega^2r^3(1-r^2))(1-r^4)^2 + r^4(-\gamma(1+r^2)\cos\alpha \\ &+ \Omega(1-r^2)\sin\alpha)(1-r^4)^3),\end{aligned} \tag{42b}$$

$$\begin{aligned}v' &= \frac{1}{2(\gamma^2(1+r^2)^4 + \Omega^2(1-r^2)^4)(1-r^4)} \\ &\times(8vru^2(\Omega^2(1-r^2)^5 - 2\gamma^2(1+r^2)^5) \\ &+ 8\gamma\Omega(3r^2u^2 + v^2 + r^4)(1-r^4)^2 \\ &+ r^2(\Omega(1-r^2)^3\cos\alpha + \gamma(1+r^2)^3\sin\alpha)(1-r^4)^2).\end{aligned} \tag{42c}$$

It should be noted that the dimensionality can be lowered (from the fourth for set of relations (41) to the third for system (42)) due to the fact that function $\theta(x)$ is defined to within a constant term, i.e., the structure of complex fields $z(x)$ and $h(x)$ (and, hence, of $Z(x, t)$ and $H(x, t)$ also) is invariant to a simultaneous phase shift by a constant. For the same reason, without loss of generality, we can set $\theta(0) = 0$. It should also be emphasized that because of boundary conditions (16) at the ends of interval $[0, L)$, we are interested only in periodic solutions to Eqs. (42) with a period coinciding with length L of the given medium. Such solutions possess an important property (translation symmetry) that allows us to choose conveniently (owing to certain arbitrariness) the position of the origin of spatial coordinate x. In addition, it can easily be seen that upon substitutions $x \to -x$, $r \to r$, $u \to -u$, and $v \to -v$, system (42) remains unchanged. In other words, relations (42) experience the involution transformation. Such properties of dependences $r(x)$, $u(x)$, and $v(x)$, as well as Eqs. (42) themselves, allow us to confine our analysis to the search for only periodic solutions $r(x)$, $u(x)$, and $v(x)$ that satisfy the following conditions:

$$\begin{gathered} r(0) = r(L), \quad u(0) = u(L) = 0, \\ v(0) = v(L) = 0. \end{gathered} \tag{43}$$

We must put in correspondence to these solutions the spatial profiles of $z(x)$ and $h(x)$, which (together with the corresponding value of parameter Ω) determine the form of stationary structures. It should also be emphasized that direct numerical calculations based on initial model (1)–(4) also support the choice of the preferred class of functions $r(x)$, $u(x)$, and $v(x)$ as most prospective for describing long-lived states with a static nonuniform distribution of the degree of phase synchronization of ensemble elements (see, for example, Fig. 1g and fragments of Figs. 2c and 2f for $t = 2000$). It should be borne in mind, however, that not all solutions to system (42) for which conditions (43) are satisfied are physically realizable. These solutions have sense only when $|r(x)| = |z(x)|$ does not exceed unity for all x on segment $[0, L)$. This requirement follows directly from the definition of local complex order parameter $Z(x, t)$. Therefore, the problem of determining stationary solutions (36) to system (12), (15) with boundary conditions (16), which was formulated at the beginning of this section, can be reduced to determining periodic trajectories of system (42), for which conditions (43) hold.

4.2. Procedure of the Search for Static Inhomogeneous States and Their Structural Analysis

Let us now consider in detail the key features of stationary regimes with a nonuniform spatial distribution of local order parameter $Z(x, t)$. In this section, we will first of all perform the procedure of the search for all existing periodic solutions to auxiliary system (42), which determine the shape of profiles of complex fields $Z(x, t)$ and $H(x, t)$ with a uniformly rotating phase. Then we single out the main distinguishing features of the family of such solutions and put them in correspondence with the pattern of spread of dynamic variables $\varphi_n(t)$, which must be realized in initial model (1)–(4) of an ensemble of nonlocally coupled nonidentical oscillator elements. Further, such states of the populations in question will be interpreted from the standpoint of mesoscopic (averaged) characteristics as well as from the standpoint of the properties of motion of individual oscillators.

Let us begin with the description of the method for determining stationary (in absolute value) states of form (36), which has been developed here based on the idea of selecting (for fixed values of Ω) of closed (and, hence satisfying conditions (43)) trajectories in phase space r, u, v of system (42) of third-order ordinary differential equations. To determine such trajectories, we have used Poincare cross section $u = 0$, $u' > 0$, constructed by numerical integration of system (42) starting from set $r(0) = r_0$, $u(0) = 0$, $v(0) = 0$, where r_0 takes its values from interval (0, 1), and detecting each event with $u = 0$, $u' > 0$, and then plotting it on the r, v plane for better visualization using a marker (Fig. 4). Our analysis (using primarily the facts described in Section 4.1) shows that stationary points of period p of the map constructed in this way correspond to the sought periodic solutions to system (42) and, hence, to symmetric spatially inhomogeneous structures with p maxima of the modulus of local order parameter $z(x, t)$. Length L of each trajectory determined in this way coincides with the length of the medium in which this state can be observed. Ultimately, for a preset Ω, we determine profile $z(x)$ that exactly repeats itself after period L determined by the choice of Ω. If necessary, dependence $h(x)$ can also be easily determined using formula (38). However, it is more important that it is always possible to reconstruct the distribution of initial dynamic variable $\varphi(x, t)$ or $\varphi_n(t)$ from local order parameter $z(x)$ with account for relation (36). Thus, we can determine various families of static inhomogeneous states of the medium of nonlocally coupled nonidentical phase oscillators. Each such family is characterized by individual $\Omega(L)$ dependence (Fig. 5) that is calculated in implicit form using the above procedure.

Before we pass to specific examples, we note that an analogous approach has already been successfully used in our previous studies [31–33] for investigating chimeras in media consisting of identical particles (i.e., $\gamma = 0$). However, in the case studied in [31–33], complications were encountered due to the presence of regions with fully synchronous elements that hampered the application of numerical procedures permitting the determination of curves reproducing themselves on a finite interval. When, however, $\gamma > 0$, it is possible to avoid problems associated with the possibility of identical coincidence of oscillator phases in the vicinity of a certain point x because the special situation with $|z(x)| = 1$ becomes unattainable. The

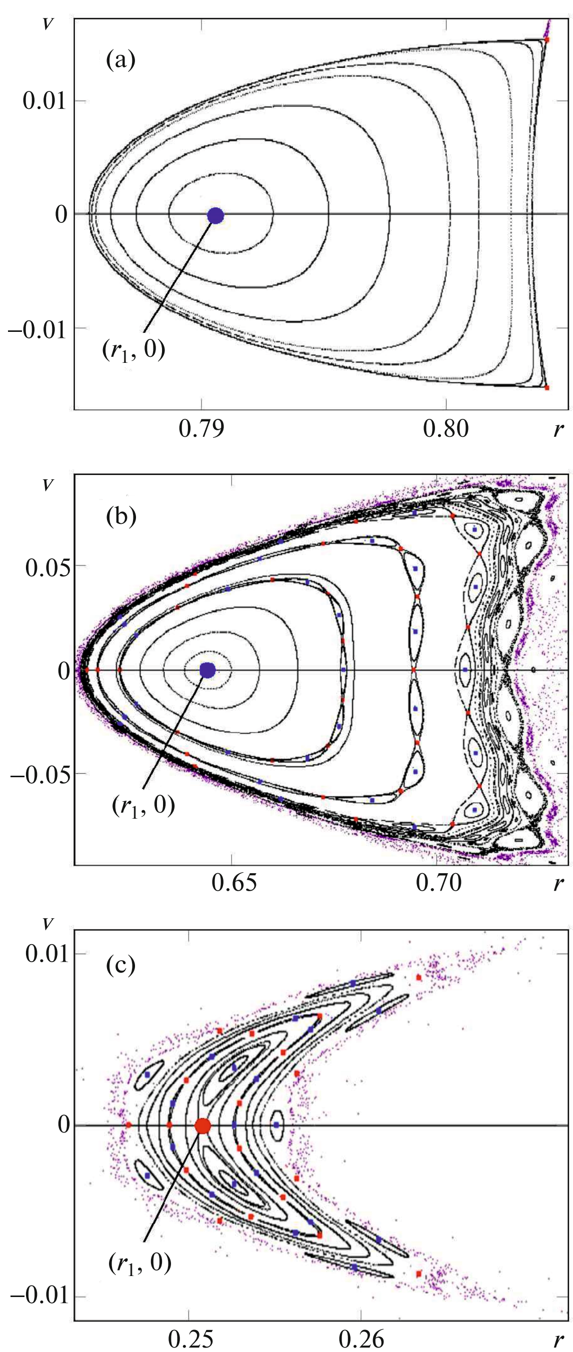

Fig. 4. Poincare map for system (42) for $\alpha = 1.457$, $\gamma = 0.020$. Conditions for the cross section: $u = 0$, $u' > 0$. Elliptical (blue symbols) and hyperbolic saddle (red symbols) stationary points: (a) $\Omega = -0.8185$; (b) $\Omega = -0.78$; (c) $\Omega = -0.647$. Stationary point $(r_1, 0)$ corresponds to nonhomogeneous solution (36)) with single maximum $|z(x)|$. Black (violet) symbols indicate trajectories that do not leave (leave) regions on the (r, v) plane, which are depicted in fragments (a–c).

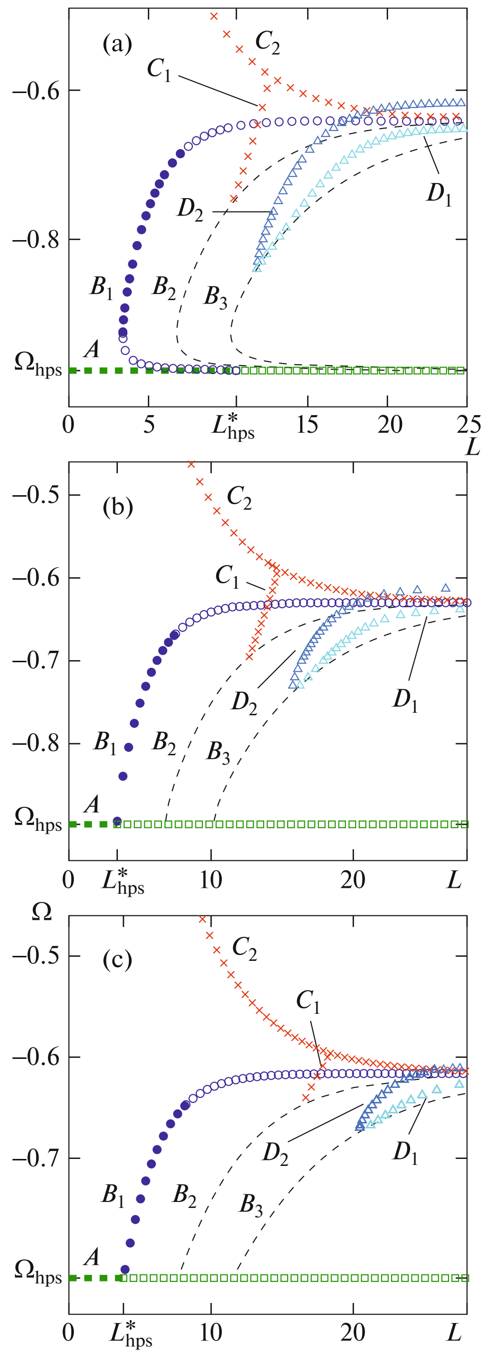

Fig. 5. Bifurcation diagram of stationary solutions (36) to Ott–Antonsen equations (12), (13) for $\alpha = 1.457$: (a) $\gamma = 0.002$, (b) $\gamma = 0.011$, and (c) $\gamma = 0.020$. Dots (A) correspond to the partially synchronous state; circles (B_1) denote inhomogeneous partially synchronous state with single maximum $|z(x)|$; crosses (C_1, C_2), with two maxima; triangles (D_1, D_2), with three maxima $|z(x)|$. Colored (empty) symbols correspond to stable (unstable) regimes. Curves B_2 and B_3 correspond to a partially synchronous state with single maximum $|z(x)|$ and with the doubled and tripled length of the medium, respectively.

requirement $|z(x)| < 1$ considerably reduces the number of initial conditions from which the construction the Poincare cross section begins. This simplifies the procedure of the search for stationary points of map and guarantees the absence of lost solutions. However, for $\gamma = 0$, analogous guaranties cannot be given because all transformations and calculations are performed with field $h(x)$ the amplitude of which is not bounded from above. On the other hand, it should be emphasized that when the value of γ responsible for the degree of spatial disorder tends to zero, stationary inhomogeneous states of form (36), which were obtained for problem (12), (15), can provide additional information on chimera solutions appearing for $\gamma = 0$ and their domains of existence.

By way of example, let us analyze the stationary points of the Poincare map for fixed values of $\alpha = 1.457$, $\gamma = 0.02$ and various Ω (see Fig. 4). For these values of parameters, there exists a homogeneous partially synchronous state of the system with $\Omega = \Omega_{\mathrm{hps}} \approx -0.81854$ and $r = r_{\mathrm{hps}} = 0.80482$.

On Poincare cross section (r, v) determined by conditions $u = 0$, $u' > 0$, this state corresponds to a stationary point with coordinates $(r_{\mathrm{hps}}, 0)$. Upon an increase in parameter Ω, this stationary point experiences bifurcation as a result of which three stationary points appear: elliptic point $(r_1, 0)$ of period $p = 1$ and two saddle points (r_2, v_2) and $(r_2, -v_2)$. In this case, closed trajectories correspond to quasi-periodic solutions to system (42) (see Fig. 4a). Stationary point $(r_1, 0)$ corresponds to inhomogeneous partially synchronous state $z = z_1(x)$ with a single maximum of the order parameter modulus $|z(x)|$.

Upon a further continuous variation of Ω, periodic points with different periods appear on invariant trajectories because of resonances (see Fig. 4b). In the case of resonance overlapping, random walk regions are formed [50]. On the Poincare map, so-called stochastic layers can be observed in such a situation near the separatrices of saddle points (see Figs. 4b and 4c). Further, for $\Omega \approx 0.648$, two elliptic points are generated from point $(r_1, 0)$, which becomes a saddle point in this case (see Fig. 4c). Pay attention to the fact that there exist a large number of stationary points with coordinated $(r, 0)$ on the Poincare map, which correspond to different stationary solutions to system (12), (15).

Upon a further increase in parameter Ω, all trajectories (except stable separatrices) near saddle point $(r_1, 0)$ rapidly leave its neighborhood. The search for a stationary point using this method is complicated because its multiplicator with the maximal absolute value considerably exceeds unity. An analogous behavior is observed in the vicinity of the remaining saddle points with a large period, which lie on axis $v = 0$. This peculiarity is associated with the increase in the length of return trajectories in the 3D phase space r, u, v.

4.3. Linear Analysis of Stability of Stationary Inhomogeneous States

In analysis of both homogeneous and twisted regimes with the degree of synchronization distributed uniformly along the entire population (see Section 3), we have established that information on the existence of states alone is insufficient for predicting possible scenarios of the long-term evolution of ensembles of nonlocally coupled phase oscillators. It is also necessary to test the corresponding spatial structures for temporal stability to small perturbations.

Following the general logical considerations that were used, in particular, in the previous section, we will perform the linear analysis of the stability of static configurations with a nonuniform local order parameter profile, which will give us a deeper understanding of the dynamics of the medium in question and cooperative processes in it. For this purpose, we linearize Ott–Antonsen integro-differential equation (12), (13) in its initial form in the vicinity of one of its stationary solutions (36) characterized by parameter Ω and length L. In accordance with the standard procedure, we write $Z(x, t)$ in form

$$Z(x,t) = (z(x) + \mathcal{Z}(x,t))e^{i\Omega t}, \tag{44}$$

where $\mathcal{Z}(x, t)$ denotes small deviations from profile $z(x)$ in complex field $Z(x, t)$, which are periodic in x [26, 31, 34]. Substituting expression (44) into Eq. (12), performing a number of transformations with account for relation (37)), and retaining only first-order terms in $\mathcal{Z}(x, t)$, we obtain

$$\frac{\partial \mathcal{Z}}{\partial t} = -(\gamma + i\Omega + h^* z)\mathcal{Z} + \frac{1}{2}(\mathcal{H} - \mathcal{H}^* z^2). \tag{45}$$

Here, $\mathcal{H}(x, t)$ and $\mathcal{Z}(x, t)$ are connected by a convolution operator with kernel (4), i.e., analogously to formula (13) expressing $H(x, t)$ in terms of $Z(x, t)$. We separate the real and imaginary components of complex function $\mathcal{Z}(x, t) = \zeta_1(x, t) + i\zeta_2(x, t)$ and write equality (45) as a system of equations in real-valued vector $\boldsymbol{\zeta}(x, t) = (\zeta_1(x, t), \zeta_2(x, t))^T$:

$$\frac{\partial}{\partial t}\boldsymbol{\zeta}(x,t) = [\hat{\mathbf{M}} + \hat{\mathbf{K}}]\boldsymbol{\zeta}(x,t), \tag{46}$$

where $\hat{\mathbf{M}}(x)$ is a multiplicative operator,

$$\hat{\mathbf{M}}\boldsymbol{\zeta}(x,t) = \begin{pmatrix} \mu_1(x) & -\mu_2(x) \\ \mu_2(x) & \mu_1(x) \end{pmatrix}\begin{pmatrix} \zeta_1(x,t) \\ \zeta_2(x,t) \end{pmatrix}, \tag{47}$$

and $\hat{\mathbf{K}}(x)$ is an integral operator:

$$\hat{\mathbf{K}}\boldsymbol{\zeta}(x,t) = \begin{pmatrix} \varkappa_{11}(x) & \varkappa_{12}(x) \\ \varkappa_{21}(x) & \varkappa_{22}(x) \end{pmatrix}\int_0^L G(x - \tilde{x})\begin{pmatrix} \zeta_1(\tilde{x},t) \\ \zeta_2(\tilde{x},t) \end{pmatrix} d\tilde{x}. \tag{48}$$

For convenience and briefness of the above representations of $\hat{\mathbf{M}}(x)$ and $\hat{\mathbf{K}}(x)$, we have introduced the following notation:

$$\begin{gathered}\mu_1(x) = -\operatorname{Re}(z(x)h^*(x)) - \gamma, \\ \mu_2(x) = -\operatorname{Im}(z(x)h^*(x)) - \Omega, \\ \varkappa_{11}(x) = (\cos\alpha - \operatorname{Re}(e^{i\alpha}z^2(x)))/2, \\ \varkappa_{12}(x) = (\sin\alpha - \operatorname{Im}(e^{i\alpha}z^2(x)))/2, \\ \varkappa_{21}(x) = \varkappa_{12} - \sin\alpha, \quad \varkappa_{22}(x) = \cos\alpha - \varkappa_{11}.\end{gathered} \tag{49}$$

Relation (46) directly implies that the behavior of small perturbations $\mathcal{X}(x, t)$ is determined by eigenvalues λ of sum $\hat{\mathbf{M}}(x) + \hat{\mathbf{K}}(x)$ of time-independent operators $\hat{\mathbf{M}}(x)$ and $\hat{\mathbf{K}}(x)$. In the full spectrum, continuous component λ_e containing a significant part of all values of λ and discrete part λ_p to which isolated points of the spectrum of λ belong are usually singled out in functional analysis. It should be noted that operator $\hat{\mathbf{K}}(x)$ is compact for any piecewise-smooth kernel $G(x)$ [34]. Due to this property, a significant part of λ_e in the set of eigenvalues λ of combination $\hat{\mathbf{M}}(x) + \hat{\mathbf{K}}(x)$ considered here coincides with the corresponding component of first term $\hat{\mathbf{M}}(x)$ in this combination. Therefore, we find that $\lambda_e = \mu_1(x) \pm i\mu_2(x)$. It can easily be verified that λ_e satisfy condition $\operatorname{Re}\lambda_e < 0$. Consequently, only the values from the point part λ_p of the λ spectrum are responsible for linear stability of spatial profile $z(x)$ (and of distribution $h(x)$ connected with it).

The results of the search for stationary inhomogeneous solutions to the Ott–Antonsen equations and of analysis of stability of the corresponding structure, which are obtained using the above methods, are combined and shown in Fig. 5. Here, dependences $\Omega(L)$ are represented for homogeneous partially synchronous states (branch A) and inhomogeneous states with one (branch B_1), two (branches (C_1 and C_2), and three (branches D_1 and D_2) maxima of amplitude $|z(x)|$ of the order parameter for stationary solutions for $\alpha = 1.457$ and several values of γ: $\gamma = 0.002$, $\gamma = 0.011$, and $\gamma = 0.020$ (Figs. 5a, 5b, and 5c, respectively). In contrast to the situation when media of identical elements are considered [26, 31–34], in the presence of a random spread (disorder) in individual frequencies of the oscillators, we can reliably calculate λ_p (at least, the values for which $\operatorname{Re}\lambda_p > 0$) using only the standard method of discretization and replacement of operators $\hat{\mathbf{M}}(x)$ and $\hat{\mathbf{K}}(x)$ by matrices with a higher dimensionality without resorting to additional modifications of such a procedure, which are necessary for determining true values of λ_p for $\gamma = 0$ (see [31–33] for details). Therefore, from the standpoint of analysis in the thermodynamic limit, we obtain one more advantage in the problem with spatial disorder (i.e., for $\gamma \neq 0$).

Each of the selected types of inhomogeneous states is marked by its own symbol. Filled colored symbols correspond to stable regimes and empty symbols, to unstable regimes. It can be seen that branch B_1 corresponding to the inhomogeneous partially synchronous regime stems from the straight line that reflects the homogeneous partially synchronous regime on the (L, Ω) plane. This occurs precisely at the instant when this regime loses its stability (i.e., at the point with abscissa $L = L^*_{\text{hps}}$, at which the solid curve changes to the dashed curve). Curves $B_2(B_3)$ correspond to the doubled (tripled) inhomogeneous states for which the length of the medium is two (three) times larger than the spatial size of structures from branch B_1, although the local complex order parameter profile coincides completely with one of distributions $z(x)$ obtained in constructing family B_1. It can easily be seen that curve B_1 contains points with such L and Ω, that the spatial formations determined for these values must be stable and, hence, represent a possible observable regime of the behavior of the system, which is stabilized during the long-term evolution. This circumstance is also confirmed by numerical simulation of the Ott–Antonsen equations. It should be noted that depending on the value of γ, transitions from a homogeneous partially synchronous regime to a cluster regime differ significantly. In the case of strong frequency detunings (large γ; Figs. 5b and 5c) the transition is soft. However, in the case of weak frequency detunings (small γ), the transition is hard, and hysteresis takes place (see Fig. 5a, region of conjugation of branches A and B_1).

With increasing parameter L, the states with one elevated and one lowered coherence regions lose their stability. An increase in the length of the ensemble also leads to regimes with a large number of clusters with different degrees of phase synchronization. In particular, an additional branch of solutions denoted by C_1 stems from branch B_2. Structures of this type are characterized by inequality $|z(x)| > 0$; consequently, the global order parameter differs from zero. Curve C_1 terminates at family C_2 that is also formed by stationary inhomogeneous regimes with $p = 2$. The main difference between states from branch C_2 and the formations with parameters lying on curve C_1 is that $|z(x)|$ for these states vanishes at two points, while macroscopic field R collected from the entire population is zero. We have encountered such a situation in comparing homogeneous partially synchronous and twisted states. If we proceed further, branch B_3 generates families D_1 and D_2, which correspond to structures with $p = 3$ and are transformed into one another. For example, with increasing L, we will register new solutions with sequentially increasing number p of maxima.

In spite of the fact that among the states discovered by us, only regimes with $p = 1$ turned out to be linear stable (in the strict sense); for some regimes with $p > 1$, the exponential growth indices are small ($\sim 10^{-3}$, 10^{-4}). Therefore, it can be expected that all static inhomogeneous structures considered here play an important role in the dynamics of the initial system. Such expectations are also confirmed by numerical calculations based on Ott–Antonsen equations (12), (15). The simulation of the initial problem shows that mesoscopic fields $Z(x, t)$ and $H(x, t)$ are transformed with a high probability to stable or weakly unstable states that are observed during long time intervals. In the next section, we will pay attention to the results of numerical calculations performed directly using initial model (1)–(4) and to the search for new (now dynamic) regimes that can appear during the breaking of static quasi-chimera structures. Concluding this section, we note that, on the one hand, degree of disorder γ leads to stabilization of stationary formations (as regards the distribution of the absolute value of the local order parameter), but on the other hand, γ affects the length of the closed trajectories of system (42) (see Fig. 5), which in turn determines in many respects the position of discrete eigenvalues λ_p of operator $\hat{\mathbf{M}}(x) + \hat{\mathbf{K}}(x)$ on complex plane (Reλ, Imλ). According to the results of above analysis, the longer the medium, the higher the probability that λ_p with Re$\lambda_p > 0$ exist. Thus, inhomogeneous states with static phase synchronization clusters are most stable in the case of intermediate values of parameter γ responsible for the spread in the individual characteristics of oscillator elements constituting the system. For example, among the situations considered in constructing Fig. 5, the formations with two clearly manifested almost nondisplaced maxima of the amplitude of field $Z(x, t)$ are observed for longest times for $\gamma = 0.011$.

5. DYNAMIC REGIMES OF LONG-TERM EVOLUTION OF A SYSTEM OF NONLOCALLY COUPLED NONIDENTICAL PHASE OSCILLATORS

In this section, we will first consider once again the regime with a static cluster synchronization pattern (see Figs. 1g and 1h) and then pass to a detailed description of the types of dynamic inhomogeneous states such as the breather cluster regime (see Figs. 1i and 1j), irregular states with a clearly manifested intermittence (see Figs. 1k and 1l), and without it (see Figs. 1m and 1n). The results described in this section were obtained by direct numerical simulation of system (1)–(4). As the initial conditions, we have specified the phase distribution reconstructed from one of profiles $z(x)$ with the corresponding value of Ω, which are determined, as has been stated in the previous section, by length L of the medium for fixed parameters α and γ. For definiteness, we choose $\alpha = 1.457$ as the phase shift parameter.

5.1. Static Cluster Synchronization

Let us first consider the situation in which the initial phase distributions are formed from the stationary inhomogeneous solutions to Ott–Antonsen equations (12), (15) with number of maxima $p = 1$. As noted above, these solutions correspond to branch B_1 on the bifurcation diagrams shown in Fig. 5. The coordinate of each amplitude maximum of complex field $Z(x, t)$ defines the position of the middle of a group with an elevated degree of phase coherence and simultaneously of the center of a cluster with frequency synchronization of oscillators (see Figs. 1g and 1h), i.e., a set of elements that have identical average frequencies $\langle\dot{\varphi}_n\rangle$. It should be noted that for identical particles ($\gamma = 0$), these two macroscopic fractions coincide and form an absolutely correlated region of the medium with $|Z(x, t)| = 1$ and $\langle\dot{\varphi}\rangle = \Omega$.

Let us consider the case with $\gamma = 0.002$ (see Fig. 5a). Then branch B_1 appears for $\Omega = \Omega^*_{\rm hps} = -0.9276$ ($L^*_{\rm hps} = 10.5141$) from a homogeneous partially synchronous regime, and the $\Omega(L)$ dependence corresponding to it is ambiguous, which is typical of the situation with bistability and hysteresis. On this branch, there exists stable interval $-0.9241 < \Omega < -0.6851$ ($3.3882 < L < 7.0$). Figure 6a shows profiles of $|z(x)|$ and $|h(x)|$, while Fig. 6b shows the corresponding distribution of instantaneous phases φ_n for $\Omega = -0.7$. Figure 6c contains the spectrum of eigenvalues λ_e and λ_p, where there exists one discrete zero eigenvalue because of the invariance of system (12), (15) to spatial shift $x \to x + x_0$; for remaining eigenvalues, condition Re$\lambda_p < 0$ holds, indicating the stability of the regime under investigation. Figure 6d shows the spatiotemporal dynamics of quantity $|Z(x, t)|$ obtained in the direct numerical simulation of system (1)–(4) with finite number of elements $N = 4096$. Figure 6e shows mean frequencies $\langle\dot{\varphi}_n\rangle$ of the oscillators. We can clearly see one cluster of elements synchronized in frequency, the main group of which is located at the middle of interval $[0, L)$, and a clearly manifested maximum in the profile of the modulus of local order parameter $Z(x, t)$. This regime for $\gamma = 0$ is transformed into a stable one-cluster chimera (see, for example, [31–33]).

Upon an increase in γ, the degree of phase coherence decreases in the whole over the entire population. The number of oscillators belonging to frequency-synchronized cluster also decreases (in percentage); i.e., the number of elements in the ensemble with identical average frequencies gradually decreases. For example, for $\gamma = 0.02$ (see Fig. 5c), the stationary inhomogeneous regime with $L = 6.5861$ and $\Omega = -0.68$ must be stable to small perturbations because the chosen length of the medium falls in the stability interval $L^*_{\rm hps} < L < L^*_1$, where $L^*_{\rm hps} = 3.83422$ and $L^*_1 = 8.232$. The results of analysis based on the approaches developed in Section 4 and direct numerical simulation of system (1)–(4) are shown in Figs. 7a–7e. Comparing these fragments in Fig. 7 with analogous panels in Fig. 6, we can easily note these features associated with a change in the degree of disorder in the medium.

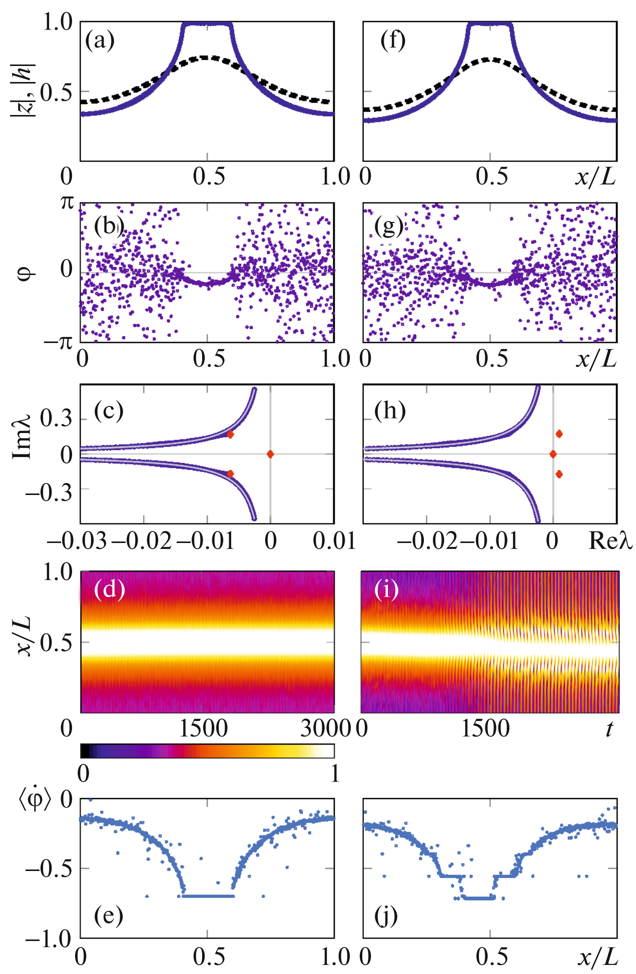

Fig. 6. (a–e) Stable inhomogeneous state for $\alpha = 1.457$, $\gamma = 0.002$, $\Omega = -0.70$, $L \approx 6.4135$. (f–j) Unstable inhomogeneous sate evolves to the breather regime for $\alpha = 1.457$, $\gamma = 0.002$, $\Omega = -0.685$, and $L = 7.0047$. The initial conditions corresponds to branch B_1 of the bifurcation diagram in Fig. 5a. (a, f) Profiles of $|z|$ (blue solid curve) and $|h|$ (black dashed curve) are determined by the method described in Section 4. (b, g) Initial distributions of phases φ_n reconstructed from local order parameter $Z(x)$. (c, h) Spectrum of λ for linear perturbations for corresponding stationary solutions $Z(x)$ to the Ott–Antonsen equations. Essential λ_e (blue circles) and point λ_p (red diamonds) components of the λ spectrum. (d, e, i, j) Results of direct numerical simulation of system (1)–(4). (d, i) Temporal behavior of the absolute value of complex field $Z(x_n, t)$. (e, j) Average frequencies $\langle\dot{\varphi}_n\rangle$ of oscillators.

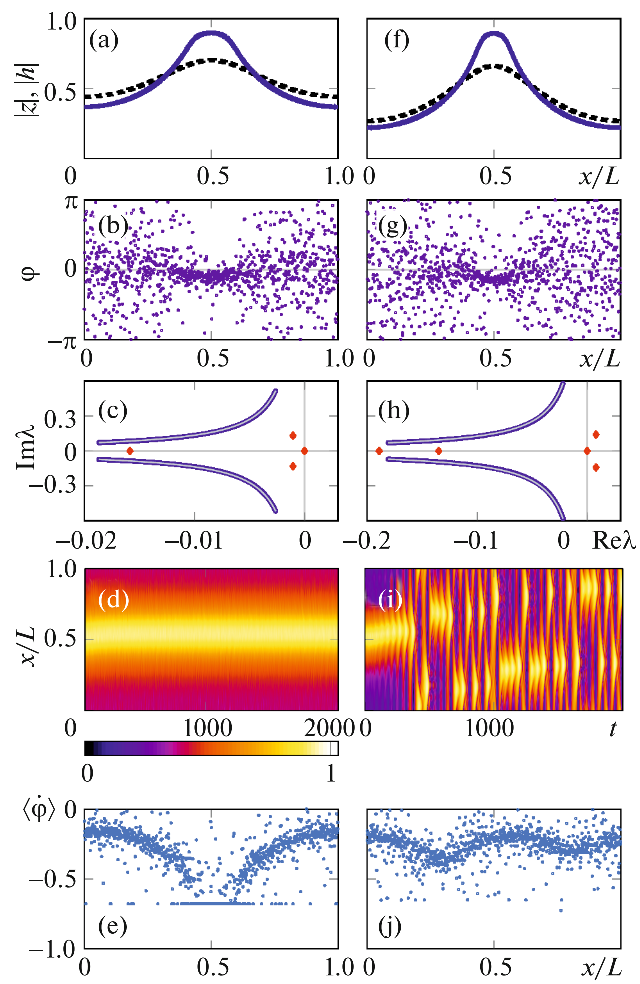

Fig. 7. Same as in Fig. 6. (a–e) Stable inhomogeneous state for $\alpha = 1.457$, $\gamma = 0.02$, $\Omega = -0.68$, $L \approx 6.5861$. (f–j) Unstable inhomogeneous state evolves to the intermittence regime for $\alpha = 1.457$, $\gamma = 0.02$, $\Omega = -0.64$, and $L \approx 8.8373$. The initial conditions correspond to branch B_1 of the bifurcation diagram in Fig. 5c.

5.2. Breather Cluster Regime

Let us now return to the case with $\gamma = 0.002$. For critical value $\Omega_1^* \approx -0.6851$ ($L_1^* \approx 7.0$), the stationary inhomogeneous regime loses its stability (see Figs. 6f–6j). In this case, two complex-conjugate eigenvalues from the spectrum of λ_p cross the imaginary axis (Fig. 6h). The system passes to the breather cluster regime, in which several frequency-synchronized clusters exist (Fig. 6j). Averaged quantities $H(x, t)$ and $Z(x, t)$ at spatial point experience periodic oscillations (Fig. 6i). It should be noted that these states in media consisting of identical elements (i.e., for $\gamma = 0$) are transformed into breather chimeras that have been detected in systems with various types of kernels determining the nonlocal coupling of kernels defined as exponentially decreasing [32, 33] and harmonic functions [26, 34], as well as in the form of a rectangle [51]. For ensembles consisting of phase oscillators with natural frequencies distributed in accordance with the Cauchy law, analogous solutions with a periodic behavior of mesoscopic fields were considered in [37, 43]. It was shown [43] that such breather regimes are realized in the widest ranges of control parameters if the value of spread parameter γ responsible for the degree of disorder is small, but differs from zero, which also holds for the situation considered here. It should also be

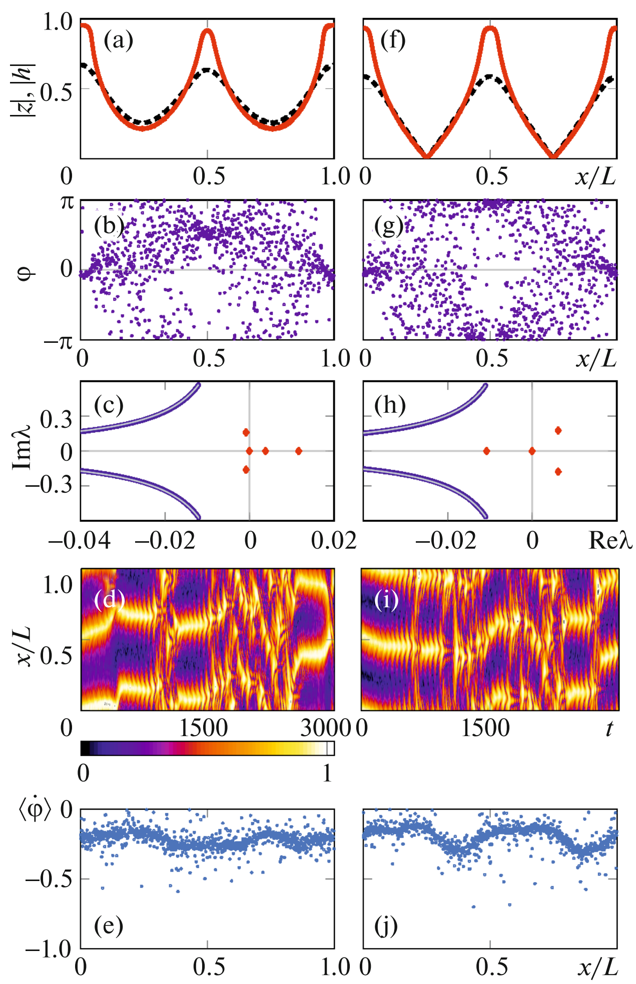

Fig. 8. Same as in Fig. 6. Unstable nonhomogeneous solutions with two $|z(x)|$ peaks (for different values of Ω and L) evolve to the intermittence regime for $\alpha = 1.457$, $\gamma = 0.011$. The initial conditions correspond to branch C_1 for $\Omega = -0.625$, $L \approx 14.1367$ (fragments (a–e)) and C_2 for $\Omega = -0.566$, $L \approx 12.7904$ (fragments f–j) of the bifurcation diagram in Fig. 5b.

noted that breather regimes are observed in 2D arrays of coupled phase oscillators [52, 53].

When $\gamma = 0.02$ and the length of the medium exceeds critical value $L_1^* = 8.232$ beginning from which the state with static cluster synchronization becomes unstable, the breather regime is registered only in a narrow interval of L values and is quite difficult to detect. However, the existence of such a regime considerably affects transient processes in the system considered here. In particular, Figs. 7f–7j clearly show that despite a substantially more complicated (irregular) behavior of movements that set in as a result of evolution of instability of the structure shown in Fig. 7f, the quasi-periodic dynamics resembling in all its features the breather cluster regime is observed on extended time intervals. Such a dynamics is interrupted by a sharp shift of the positions of regions with elevated and lowered phase coherence in space, after which it is restored again (Fig. 7i). Such alteration of prolonged oscillations of the structure of mesoscopic fields and rapid (jumpwise) changes occurring during short (on the scales of numerical calculations) time intervals can be interpreted as the intermittence effect. This phenomenon is one of the mechanisms of transition to developed turbulence, which in fact occurs upon a further increase in the length of the medium. The system begins to demonstrate the spatiotemporal dynamics with an irregular behavior of averaged complex fields $Z(x, t)$ and $H(x, t)$, which will be considered below.

5.3. Irregular Regimes

It should be emphasized once again that in all situations considered here, when the distribution of the complex order parameter modulus has one or several peaks and never turns zero, the breaking of regular (as regards mesoscopic fields) static inhomogeneous states always occurs in accordance with analogous scenarios. Two complex-conjugate values belonging to the discrete spectrum of λ_p intersect the imaginary axis, indicating the oscillatory nature of instability. In this case, we can trace a direct analogy with the Andronov–Hopf bifurcation [54]. In particular, this interpretation is confirmed by the fact that for certain combinations of quantities α, γ, and L, the transition to breather cluster regimes can be detected reliably, and only then the breaking of states corresponding to stationary quasi-chimera solutions to Ott–Antonsen equations (12), (15) terminates upon an increase in length L of the medium by the stabilization of complex dynamic regimes distinguished by the drift and abrupt shifts of the positions of regions with elevated and lowered degree of phase coherence. It is worth noting that in most cases (on the one hand, two quite extended populations, and on the other hand, populations having a finite size), the number of local extrema in the spatial dependences of amplitudes of averaged complex fields at each instant is conserved (Figs. 8d and 8i).

In this section, we first single out and consider in greater detail the main features of irregular inhomogeneous regimes in the situation when $\gamma = 0.011$ and the initial conditions for elements of the ensemble are formed using stationary solutions to Ott–Antonsen equations (12), (15), for which $p = 2$, and the corresponding branches are marked in Fig. 5b as C_1 and C_2. It can be concluded from the above arguments and from the description given below that other irregular regimes (evolving from static cluster states with other number of maxima of $|z(x)|$) are also possible. Figures 8a, 8f and 8b, 8g show typical profiles $|z(x)|$ of the local order parameter and distributions of phases φ_n associated with them. The corresponding spectra of eigenvalues λ of composite operator $\hat{\mathbf{M}}(x) + \hat{\mathbf{K}}(x)$ of linear stability problem (46) are shown in Figs. 8c and 8h. It can easily be seen that among eigenvalues λ, there are such that $\mathrm{Re}\lambda > 0$ (it should be noted by the way that $\mathrm{Re}\lambda \sim 10^{-2}$). Therefore, these regimes are weakly unstable, and in direct numerical simulation, ensemble (1)–(4) of phase oscillators demonstrates a transition to a complex spatiotemporal dynamics (of complex mesoscopic fields also). However, it can clearly be seen that over quite long time intervals, the dynamics returns to states in which we can single out two quasi-static regions with a high degree of coherence and two (also quasi-static) regions with practically asynchronous behavior of oscillators (Figs. 8d and 8i). At the ends of long time intervals, the distribution of the $Z(x, t)$ amplitude stars swinging and passing from the close structure to the stationary structure via oscillations, which can be explained precisely by the oscillatory evolution of instability. Therefore, the system demonstrates the intermittency of regular and chaotic regimes. This is due to the fact that among our solutions to Eqs. (12), (15) corresponding to branches C_1 and C_2 in Fig. 5, there exist weakly unstable distributions that can be put in correspondence to relatively simple transient long-lived regimes of motion. In this case, it is impossible to single out clusters of partially synchronous oscillators on the profile of mean frequencies $\langle\dot{\varphi}_n\rangle$ (see Figs. 8e and 8j) because over quite long time interval (averaging interval), each element can "visit" both regions with a high degree of phase coherence and almost asynchronous regions of the medium. For this reason, the mean frequencies have an almost uniformly noisy profile positioned close to the curve the shape of which exhibits, however, traces of structural singularities because the population is located for quite a long time in the vicinity of one of weakly unstable formations considered in Section 4.

If the $|z(x)|$ profile determining the initial values is strongly unstable, the system demonstrates chaotic spatial dynamics that is not interrupted now by a transition to quasi-static regular structures. By way of example, we consider the case with $\gamma = 0.02$ for unstable inhomogeneous states with three $|z(x)|$ peaks. Figures 9a–9e correspond to the solution lying on branch D_1, while Figs. 9f–9j correspond to the solution located on branch D_2. Here, the states corresponding to the regime with three regions of elevated phase coherence are broken quite rapidly, and the local order parameter begins demonstrating irregular dynamics (Fig. 9d and 9i). The distribution of average frequencies $\langle\dot{\varphi}_n\rangle$ in this case turns out to be uniformly noised (like in the case of intermittence). However, in contrast to Figs. 8e and 8j, the values of $\langle\dot{\varphi}_n\rangle$ in Figs. 9e and 9j are distributed almost over a straight line with the same spread, indicating the absence of significant differences between the spatial points of the medium after averaging over time.

Thus, in system (1)–(4) of nonidentical nonlocally coupled phase oscillators for $\gamma < \cos\alpha/2$ and $\gamma \gtrsim \cos^3\alpha$, beginning from the critical value of length L of the medium, stable inhomogeneous states with a regular behavior of averaged fields are not observed. Instead of these states, complex spatiotemporal regimes with a chaotic dynamics of order parameter $Z(x, t)$ of two types are realized. In one case, intermittency takes place, in which quite long time intervals alternate with quasi-static distributions of mesoscopic characteristics of the ensemble and with a relatively fast shift of regions with elevated and lowered degrees of synchronization, while in the other case, a pure turbulent regime is realized.

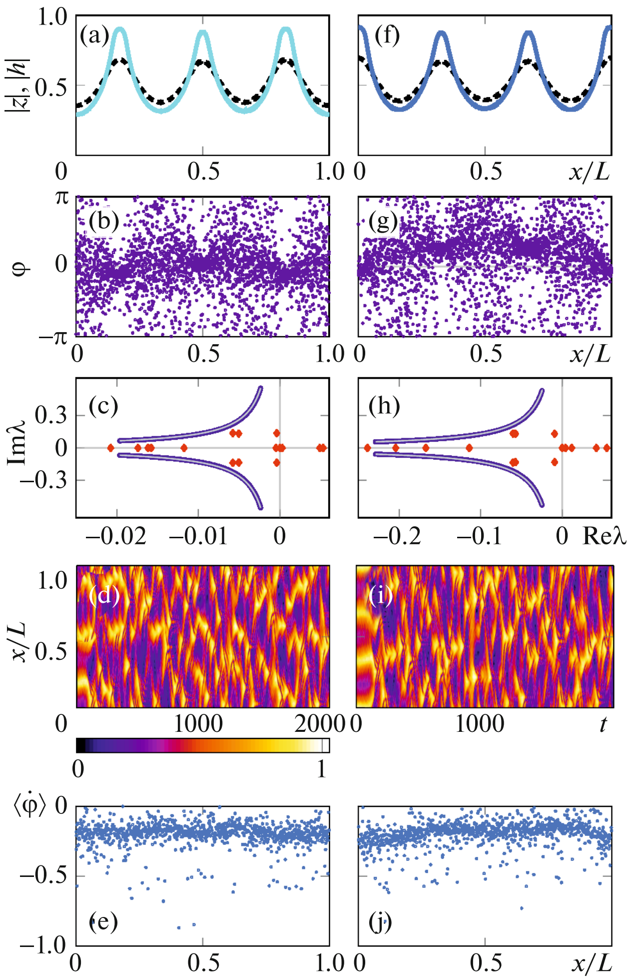

Fig. 9. Same as in Fig. 6. Unstable nonhomogeneous solutions with three $|z(x)|$ peaks (for different values of Ω and L) evolves to the turbulent regime for $\alpha = 1.457$, $\gamma = 0.020$. The initial conditions correspond to branches D_1 for $\Omega = -0.66$, $L \approx 21.9922$ (fragments (a–e)) and D_2 for $\Omega = -0.66$, $L \approx 20.7145$ (fragments (f–j)) of the bifurcation diagram in Fig. 5c.

6. CONCLUSIONS

Let us briefly summarize the results and formulate the main conclusion of this study. We have considered an ensemble consisting of a large number of nonlocally coupled nonidentical phase oscillators that are distributed uniformly on a segment with periodic boundary conditions. We assume that the natural frequencies are specified independently at random in accordance with the Lorentz distribution, and the interaction between the oscillators decreases in accordance with an exponential law. It should be noted that such a configuration is equivalent to the situation when the elements are located on a ring. The main parameters of such a system are the phase shift, which determines the type of coupling (attracting, neutral, or repulsing); the half-width of the distribution of natural frequencies, which determined the degree of their nonuniformity; and the length of the oscillator medium. This study is mainly aims at analysis and classification of the spatiotemporal structures appearing during the long-term evolution of the given ensemble in a wide range of the values of the above parameters.

Using the averaging procedure, we have obtained the dynamic Ott–Antonsen equation for the local complex order parameter characterizing the degree of phase correlation of elements in a small neighborhood of an arbitrary point in the oscillator medium under investigation. Using this equation, we have primarily determined stationary (uniformly rotating) regimes with the modulo constant value of the local order parameter. It has been established that among such states, we can single out two types, homogeneous and twisted states. Further, we have tested their stability using analysis of the eigenvalue spectrum of the corresponding linearized equations. It has been demonstrated that for large values of the half-width of the natural frequency distribution function, only a fully asynchronous regime with zero mean field is realized. If, however, the half-width of the random spread becomes smaller than a certain threshold value, this state loses its stability, and both homogeneous and twisted partially synchronous regimes can be observed depending on the size of the medium and the phase shift.

Using the fact that the interaction between the elements decreases exponentially, the Ott–Antonsen integro-differential equation has been transformed to a self-consistent system of equations in partial derivatives. This enabled up to propose a method for the effective search for stationary (uniformly rotating) inhomogeneous spatial structures, which are transformed into chimera states in the limit of identical elements. The main idea of this method is the construction of closed trajectories in the phase space for an auxiliary system of third-order ordinary differential equation. It should be noted that such periodic solutions can easily be put in correspondence with stationary points of a 2D map. Having found examples of nonuniform profiles of local complex order parameter and having reconstructed the phase distributions from these profiles, we have tested the stability of the resultant states by calculating the linear perturbation spectrum and using direct numerical simulation. To perform such analysis, we have developed and adapted, in particular, the procedure for calculating the continuous and discrete components of the eigenvalue spectrum of the Ott–Antonsen integro-differential equation linearized around one of stationary formations.

Ultimately, it has been established that among inhomogeneous states with a static distribution of regions with elevated and lowered degree of synchronization, only the regimes for which the local order parameter profile has only one maximum is stable. However, among other structures determined in this study, weakly unstable (transient) formations are encountered. Using direct numerical simulation based on the initial system, we have confirmed these conclusions and shown that the quasi-chimera (both asymptotic and transient) regimes of rotation under investigation play an important role in the dynamics of an ensemble of a large number of nonidentical nonlocally coupled phase oscillators with the exponential type of interaction because some of them are stabilized and subsequently do not break, while others appear in the form of transient long-lived processes between intervals with a complex irregular behavior of averaged fields. In addition, apart from such an intermittence of regular and chaotic collective movements for extended media, numerical calculations have made it possible to single out and describe such states of the long-term evolution of the system in question as a breather cluster synchronization and a developed turbulent regime.

FUNDING

This study was supported by the Russian Science Foundation (project no. 19-12-00367) (Sections 1 and 2), the Ministry of Science and Higher Education of the Russian Federation (project no. 0729-2020-0036) (Section 3), and by the Russian Foundation for Basic Research (project no. 19-52-12053) (Sections 4 and 5). AP was supported by German Science Foundation (grant PI 220/22-1).

REFERENCES

1. G. V. Osipov, J. Kurths, and Ch. Zhou, *Synchronization in Oscillatory Networks* (Springer, Berlin, 2007).
2. V. S. Afraimovich, V. I. Nekorkin, G. V. Osipov, and V. D. Shalfeev, *Stability, Structures and Chaosin Nonlinear Synchronization Networks* (World Scientific, Singapore, 1994).
3. J. Pantaleone, Am. J. Phys. **70**, 992 (2002).
4. S. Chhabria, K. A. Blaha, F. D. Rossa, and F. Sorrentino, Chaos **28**, 111102 (2018).
5. J. Machowski, J. W. Bialek, and J. R. Bumby, *Power System Dynamics: Stability and Control* (Wiley, New York, 2002).
6. P. J. Menck, J. Heitzig, J. Kurths, and H. J. Schellnhuber, Nat. Commun. **5**, 3969 (2014).
7. S. Ryu, W. Yu, and D. Stroud, Phys. Rev. E **53**, 2190 (1996).

8. Z. Zheng, B. Hu, and G. Hu, Phys. Rev. E **57**, 1139 (1998).
9. S. Homma and S. Takeno, Prog. Theor. Phys. **72**, 4 (1984).
10. S. Takeno and S. Homma, Prog. Theor. Phys. **77**, 3 (1987).
11. A. Pikovsky, M. Rosenblum, and J. Kurths, *Synchronization: A Universal Concept in Nonlinear Science* (Cambridge Univ. Press, Cambridge, 2001).
12. Y. Kuramoto, *Chemical Oscillations, Waves, and Turbulence* (Springer, Berlin, 1984).
13. A. Pikovsky and M. Rosenblum, Chaos **25**, 097616 (2015).
14. E. Brown, J. Moehlis, and P. Holmes, Neural Comp. **16**, 4 (2004).
15. C. R. Laing, J. Math. Neurosci. **8**, 4 (2018).
16. J. Acebron, L. Bonilla, C. P. Vicente, F. Ritort, and R. Spigler, Rev. Mod. Phys. **77**, 137 (2005).
17. F. A. Rodrigues, T. K. D. Peron, P. Ji, and J. Kurths, Phys. Rep. **610**, 1 (2016).
18. S. Gupta, A. Campa, and S. Ruffo, *Statistical Physics of Synchronization* (Springer Int., Switzerland, 2018).
19. S. Watanabe and S. H. Strogatz, Phys. Rev. Lett. **70**, 2391 (1993).
20. E. Ott and T. M. Antonsen, Chaos **18**, 037113 (2008).
21. E. Ott and T. M. Antonsen, Chaos **19**, 023117 (2009).
22. B. Pietras and A. Daffertshofer, Chaos **26**, 103101 (2016).
23. D. Chowdhury and M. C. Cross, Phys. Rev. E **82**, 016205 (2010).
24. M. J. Panaggio and D. M. Abrams, Nonlinearity **28**, R67 (2015).
25. N. Yao and Z. Zheng, Int. J. Mod. Phys. B **30**, 1630002 (2016).
26. O. E. Omel'chenko, Nonlinearity **31**, R121 (2018).
27. S. Majhi, B. K. Bera, D. Ghosh, and M. Perc, Phys. Life Rev. **28**, 100 (2019).
28. E. Schöll, A. Zakharova, and R. G. Andrzejak, *Chimera States in Complex Networks* (Frontiers Media SA, Lausanne, 2020).
29. E. Schöll, Eur. Phys. J. Spec. Top. **225**, 891 (2016).
30. A. E. Motter, Nat. Phys. **6**, 164 (2010).
31. L. Smirnov, G. Osipov, and A. Pikovsky, J. Phys. A: Math. Theor. **50**, 08LT01 (2017).
32. M. I. Bolotov, L. A. Smirnov, G. V. Osipov, and A. S. Pikovsky, JETP Lett. **106**, 393 (2017).
33. M. I. Bolotov, L. A. Smirnov, G. V. Osipov, and A. Pikovsky, Chaos **28**, 045101 (2018).
34. O. E. Omel'chenko, Nonlinearity **26**, 9 (2013).
35. M. Wolfrum, O. E. Omel'chenko, S. Yanchuk, and Y. L. Maistrenko, Chaos **21**, 013112 (2011).
36. G. B. Ermentrout, SIAM J. Appl. Math. **52**, 1665 (1992).
37. C. R. Laing, Phys. D (Amsterdam, Neth.) **238**, 1569 (2009).
38. C. R. Laing, Chaos **52**, 013113 (2009).
39. W. S. Lee, J. G. Restrepo, E. Ott, and T. M. Antonsen, Chaos **21**, 023122 (2011).
40. G. S. Medvedev and X. Tang, J. Nonlin. Sci. **25**, 1169 (2015).
41. O. E. Omel'chenko, M. Wolfrum, and C. R. Laing, Chaos **24**, 023102 (2014).
42. M. Wolfrum, S. V. Gurevich, and O. E. Omel'chenko, Nonlinearity **29**, 257 (2016).
43. O. E. Omel'chenko, Chaos **30**, 043103 (2020).
44. D. Wiley, S. Strogatz, and M. Girvan, Chaos **16**, 015103 (2006).
45. T. Girnyk, M. Hasler, and Y. Maistrenko, Chaos **22**, 013114 (2012).
46. D. Bolotov, M. Bolotov, L. Smirnov, G. Osipov, and A. Pikovsky, Regular Chaotic Dyn. **24**, 717 (2019).
47. Y. Kuramoto and D. Battogtokh, Nonlin. Phenom. Complex Syst. **5**, 380 (2002).
48. I. N. Pesin, *Classical and Modern Integration Theories,* Vol. 8 of *Probability and Mathematical Satistics* (Academic, New York, 1970).
49. W. Eckhaus, *Studies in Nonlinear Stability Theory* (Springer, Berlin, 1965).
50. F. C. Moon, *Chaotic Vibrations: An Introduction for Applied Scientists and Engineers* (Wiley-VCH, 2004).
51. Y. Suda and K. Okuda, Phys. Rev. E **97**, 042212 (2018).
52. J. Xie, E. Knobloch, and H.-C. Kao, Phys. Rev. E **92**, 042921 (2015).
53. O. E. Omel'chenko, M. Wolfrum, and E. Knobloch, SIAM J. Appl. Dyn. Syst. **17**, 97 (2018).
54. Y. A. Kuznetsov, *Elements of Applied Bifurcation Theory* (Springer, New York, 1995).

Translated by N. Wadhwa